NASA TECHNICAL TRANSLATION

NASA TT F-702

NASA TT F-702
c. 1

TECH LIBRARY KAFB, NM
0069050

LOAN COPY: RETURN TO
AFWL (DOGL)
KIRTLAND AFB, N. M.

THE CALCULATION OF THE PRESSURE DISTRIBUTION ON A CASCADE OF THICK AIRFOILS BY MEANS OF FREDHOLM INTEGRAL EQUATIONS OF THE SECOND KIND

by E. Martensen

No. 23, Max-Planck-Institute for Fluid Research and Aerodynamic Experimental Station, Göttingen, 1959

NATIONAL AERONAUTICS AND SPACE ADMINISTRATION • WASHINGTON, D. C. • JULY 1971

TECH LIBRARY KAFB, NM
0069050
NASA TT F-702

THE CALCULATION OF THE PRESSURE DISTRIBUTION ON A CASCADE OF THICK AIRFOILS BY MEANS OF FREDHOLM INTEGRAL EQUATIONS OF THE SECOND KIND

By E. Martensen

Aerodynamic Experimental Station, Göttingen

Translation of "Die Berechnung der Druckverteilung an Dicken Gitterprofilen mit Hilfe von Fredholmschen Integralgleichungen Zweiter Art." Nr. 23, Mitteilungen aus dem Max-Planck-Institut für Strömungsforschung und der Aerodynamischen Versuchsanstalt, Göttingen, 1959

NATIONAL AERONAUTICS AND SPACE ADMINISTRATION

For sale by the National Technical Information Service, Springfield, Virginia 22151
$3.00

THE CALCULATION OF THE PRESSURE DISTRIBUTION ON A CASCADE OF THICK AIRFOILS BY MEANS OF FREDHOLM INTEGRAL EQUATIONS OF THE SECOND KIND

by

E. Martensen

Aerodynamic Experimental Station, Göttingen

ABSTRACT

Two independent linear integral equations of the second kind with continuous kernels are derived for the exact potential theory for the velocity distribution on a cascade of thick airfoils. It is shown that the corresponding homogeneous integral equations possess one and only one nontrivial solution, so that one knows the general results on the basis of the Fredholm theorems. In the limiting case of infinite separation between airfoils the equations reduce to the familiar expressions for single airfoils. In the light of the periodicity properties which are present, one may develop a numerical calculation technique based on the solution from a system of linear equations. By selecting an adequately large number of unknowns, the desired accuracy is obtained. Examples are shown correlating the theory with an exact known solution and with measurements.

TABLE OF CONTENTS

Section		Page
1	INTRODUCTION	1
2	GEOMETRY OF THE CASCADE	6
3	DERIVATION OF THE INTEGRAL EQUATION FOR A SINGLE AIRFOIL ($t = \infty$)	6
4	THE PARAMETRIC REPRESENTATION OF $\mathfrak{L}_0$	11
5	EXISTENCE AND MULTIPLICITY OF THE SOLUTION OF THE INTEGRAL EQUATION OF THE SECOND KIND	14
6	TRANSFORMATION OF THE INTEGRAL EQUATION OF THE FIRST KIND TO AN EQUATION OF THE SECOND KIND, AND THE SOLUBILITY OF THE LATTER	15
7	DERIVATION OF THE INTEGRAL EQUATION FOR A CASCADE OF AIRFOILS	17
8	EXISTENCE AND MULTIPLICITY OF THE SOLUTIONS FOR THE INTEGRAL EQUATIONS OF THE SECOND KIND FOR A CASCADE OF AIRFOILS	22
9	NUMERICAL AUXILIARIES	26
10	PRACTICAL CALCULATION PROCEDURE	27
11	EXAMPLE FOR 2N = 24 CONTOUR POINTS	30
REFERENCES		34
TABLES		35
FIGURES		44

1. INTRODUCTION

The potential flow about a two-dimensional body can be represented by an arrangement of singularities in the enclosed region and on its boundaries in numerous ways. These singularities can occur at points or lines, or their combinations. The question now is which one of these unlimited possibilities is the simplest. One is therefore led to a field which vanishes identically inside the region and has a jump at the wall, which gives rise to a vortex distribution corresponding to the local velocity distribution. Until recently only approximate treatments for these methods were published because of the high calculating costs. These singularities may be vortices, sources and/or vortex-source combinations arbitrarily arranged in points and/or lines. An example of the use of this method is for the flow around airfoils which has been accomplished by placing these singularities over its chord. However, a more suitable, simple and elegant singularity method that agrees with the exact solution of the classical flow problem for thick airfoils, which vanishes identically in the field, consists of covering the boundary with a vortex distribution, for the following reasons:

1. The velocity distribution can be substituted for the vortex distribution since both views are identical to each other. While for the previous case of including singularities in the field theoretical considerations and practical calculations are required in order to establish the relationship between the vortex distribution and the velocity distribution.
2. Existence and continuity of the solution may be established on

the basis of Fredholm's theory, utilizing continuity and differentiability properties. For integral equations of the first kind with singular kernels, such conclusions are not available.

3. The numerical procedure for solving the above integral equations of the second kind with continuous and, in the present case, periodic kernels, reduces to a summation procedure. In contrast, the singularity for the integral equation of the first kind gives rise to a characteristic difficulty.

The method of covering the boundary with vortices has been presented previously by Korn in a textbook [5]. Later Prandtl [6] expounded on this idea as follows.

> Imagine the interior of a body replaced by fluid at rest, of a pressure $p_0 + q_1$, as is present at the stagnation point. At the boundary a vortex sheet produces a velocity jump of magnitude v. This vortex sheet is the desired bound vortex system.

Prager [7] establishes, by the exclusive use of this method, a Fredholm integral equation of the second kind for the velocity distribution around thick single airfoils and obtains good numerical results. He used an integration procedure of Nyström [8] and the Tschebyscheff quadrature formula. The rapid development of computer mathematics since Prager's original work has increased the usefulness of his approach. The greatly increased storage capacities of the presently used electronic computers permit improving the accuracy of the calculations to any desired extent. In reference to the work of Föttinger [9], Prager has demonstrated the inferiority of a source distribution over the boundary as compared with a vortex distribution. Goldstein and Jerison [10] adapt this idea to a

cascade of airfoils. They determined the airfoil contour for a given velocity distribution (indirect problem). This point of view is used advantageously for the derivation of the fundamental equations, even though the specific Fredholm theory is not needed. Finally Isay [11] has also treated a cascade of thick airfoils by using vortex distributions over their boundaries. No use is made in this work of the identity of the vortex distribution and the velocity distribution since the latter is provided from the vortex distribution by means of an integration formula. Nor is the pertinent integral equation of the first kind with a singular kernel converted to an integral equation of the second kind with a continuous kernel. So Fredholm's theorems are not applicable. Existence of the solution can be established only by insistence on the additional condition for the cascade geometry (t equals the pitch)

$$\frac{1}{4\pi^2}\int_0^{2\pi}\int_0^{2\pi} H(\phi, \psi, t)^2 \, d\phi \, d\psi < 1$$

Inasmuch as this limitation does not arise in the treatment of the flow problem using Fredholm integral equations of the second kind, an example using an ellipse (thickness ratio $0 < \varepsilon < 1$) will be given for illustration. This example cannot be treated by the Isay procedure. First, in using the parametric representation for the ellipse one obtains the following formula [11]

$$H(\phi, \psi; \infty) = \frac{(1 - \varepsilon^2) \sin(\phi + \psi)}{(1 + \varepsilon^2) - (1 - \varepsilon^2) \cos(\phi + \psi)} .$$

For the evaluation of this double integral we now examine the integral equation

$$f(\phi) - \frac{\lambda}{2\pi} \int_0^{2\pi} H(\phi, \psi, \infty)\, f(\psi)\, d\psi = 0$$

and seek nontrivial solutions which are square integrable from 0 to 2π. Since

$$\frac{1}{2\pi} \int_0^{2\pi} H(\phi, \psi, \infty)\, d\phi$$

$$= \frac{1}{2\pi} \left[\ln((1 + \varepsilon^2) - (1 - \varepsilon^2) \cos(\phi + \psi))\right]_0^{2\pi} = 0 ,$$

the condition

$$\frac{1}{2\pi} \int_0^{2\pi} f(\phi)\, d\phi = 0$$

must necessarily be obeyed. By the integration in the complex plane (residue method) one can easily confirm that

$$\frac{1}{2\pi} \int_0^{2\pi} H(\phi, \psi, \infty)\, e^{i\nu\psi}\, d\psi = i\left(\frac{1 - \varepsilon}{1 + \varepsilon}\right)^{\nu} e^{i\nu\phi} ,$$

$$\nu = 1, 2, 3, \ldots .$$

There result the eigenvalues

$$\lambda_\nu = \frac{\nu}{|\nu|} \left(\frac{1 + \varepsilon}{1 - \varepsilon}\right)^{|\nu|} , \quad \nu = \pm 1, \pm 2, \pm 3, \ldots ,$$

associated with the eigenfunctions

$$f_\nu(\phi) = \cos \nu\phi + \sin \nu\phi , \quad \nu = \pm 1, \pm 2, \pm 3, \ldots .$$

Since this system of functions is complete, it follows from the theory of integral equations of the second kind that:

$$\sum_\nu \frac{1}{\lambda_\nu^2} = \frac{1}{4\pi^2} \int_0^{2\pi} \int_0^{2\pi} [H(\phi, \psi, \infty)]^2\, d\phi\, d\psi .$$

Hence the earlier stated inequality reduces to

$$2 \sum_{\nu=1}^{\infty} \left(\frac{1 - \varepsilon}{1 + \varepsilon}\right)^{2\nu} = \frac{(1 - \varepsilon)^2}{2\varepsilon} < 1 .$$

But this is equivalent to saying that all elliptical contours with a thickness ratio

$$0 < \varepsilon \leq 2 - \sqrt{3} = 0.26795$$

(interesting cases) are excluded by Isay's condition.

In the following, the Prager integral equation for a single airfoil [7] will be derived in a simplified fashion and the treatment for a cascade of airfoils will be formulated using the work of Goldstein and Jerison [10]. Next, Isay's singular integral equation of the first kind, (to be derived by an alternate method), will be converted to a Fredholm integral equation of the second kind with a continuous kernel. Thus two Fredholm equations of the second kind will be available for calculating the pressure distribution for a cascade of thick airfoils. Which of the two is more suitable for numerical calculations cannot be determined in general. It will depend on the specifics of the problem. Particular emphasis will be placed in the degenerate case of a single eigenvalue since the Fredholm theory is applied to this first and it permits the development of a suitable calculation scheme. This involves essentially the solution of a system of linear equations with three inhomogeneous terms corresponding to the two main flow directions and the free circulation. A series of examples will be carried out for illustration using the Göttingen electronic computer G2.

2. GEOMETRY OF THE CASCADE

The cascade is described by congruent contours $\mathcal{L}_0$, $\mathcal{L}_1$, $\mathcal{L}_{-1}$, ... , which are arranged at equal intervals t in the y-direction (Fig. 1). The contour $\mathcal{L}_0$ satisfies (and so do $\mathcal{L}_1$, $\mathcal{L}_{-1}$, ...) continuity and differentiability conditions, to be specified later. Essentially one prohibits discontinuities in the tangent, and curvature and the third and fourth derivatives, as well as corners, cusps and double values.

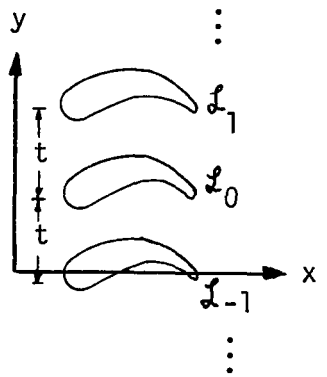

Figure 1

3. DERIVATION OF THE INTEGRAL EQUATION FOR A SINGLE AIRFOIL (t = ∞)

It is desired to obtain the velocity distribution (as well as the pressure distribution) on the contour for a simply connected contour $\mathcal{L}_0$ with no double points. The free stream velocity is given by $\vec{w}_\infty$ in an incompressible potential flow (see Figure 2). The components of this flow are related to the stream function Ψ by

$$w_x = \Psi_y, \qquad w_y = -\Psi_x , \tag{1}$$

or equivalently

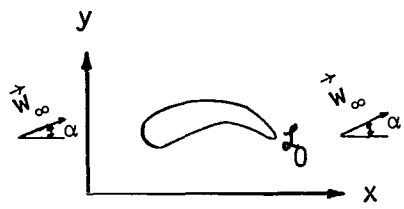

Figure 2

$$|\vec{w}| = \left|\frac{\partial \Psi}{\partial n}\right| \tag{2}$$

holds; the flow direction is at 90° counterclockwise to the direction of decreasing Ψ (Figure 3).

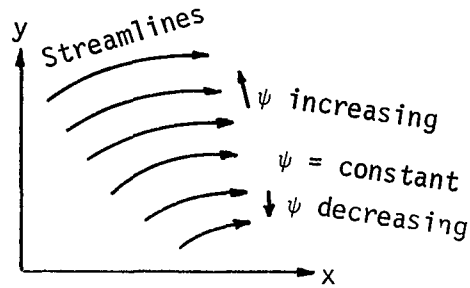

Figure 3

ψ itself obeys Laplace's equation

$$\Delta \Psi = 0 \ , \tag{3}$$

in accordance with the vortex free nature of the field (1). The problem

is to determine a flow field that goes to $\vec{w}_\infty$ at infinity and has $\mathcal{L}_0$ as a streamline, i.e., a function Ψ that has the following properties:

I. $\Delta\Psi = 0$ outside $\mathcal{L}_0$,

II. $\left(\frac{\partial\Psi}{\partial y}\right)_\infty = v_\infty \cos\alpha$, $\quad -\left(\frac{\partial\Psi}{\partial x}\right)_\infty = v_\infty \sin\alpha$,

III. Ψ = constant along the outer boundary of $\mathcal{L}_0$.

One assumes the solution

$$\Psi(x, y) = v_\infty(y \cos\alpha - x \sin\alpha) + \frac{1}{2\pi}\int_{\mathcal{L}_0} v \ln\frac{1}{r}\, ds + \text{constant} \tag{4}$$

This satisfies requirements I and II with a surface distribution along $\mathcal{L}_0$ equal to v. When crossing $\mathcal{L}_0$ the values of the normal derivatives (n is the outer normal) jump as follows:

$$\left(\frac{\partial\Psi}{\partial n}\right)_o - \left(\frac{\partial\Psi}{\partial n}\right)_{\mathcal{L}_0} = -\frac{v}{2} \tag{5}$$

$$\left(\frac{\partial\Psi}{\partial n}\right)_{\mathcal{L}_0} - \left(\frac{\partial\Psi}{\partial n}\right)_i = -\frac{v}{2}\,. \tag{6}$$

These are proven in Courant and Hilbert [4] subject to the condition that the contour $\mathcal{L}_0$ is four times continuously differentiable. However, this investigation will not be concerned with an exploration whether these conditions are also necessary or whether they may be mitigated. The integral which appears in $(\partial\Psi/\partial n)_{\mathcal{L}_0}$ is interpreted as a Cauchy principal value. The tangential derivative remains constant in crossing $\mathcal{L}_0$;

$$\left(\frac{\partial\Psi}{\partial t}\right)_o - \left(\frac{\partial\Psi}{\partial t}\right)_{\mathcal{L}_0} = 0 \tag{7}$$

$$\left(\frac{\partial \Psi}{\partial t}\right)_{\mathcal{L}_0} - \left(\frac{\partial \Psi}{\partial t}\right)_i = 0 \ . \tag{8}$$

There arise two possibilities for the distribution v to conform to condition III. In one case, one is lead to an integral equation of the first kind for v, in the second case to one of the second kind.

The first is obtained by setting

$$\left(\frac{\partial \Psi}{\partial t}\right)_o = 0 \ . \tag{9}$$

Use of (4) and (7) then establishes the following integral equation:

$$-\frac{1}{\pi}\frac{\partial}{\partial t}\int_{\mathcal{L}_0} v \ln\frac{1}{r}\,ds = 2v_\infty \frac{\partial}{\partial t}(y\cos\alpha - x\sin\alpha) \ . \tag{10}$$

Before investigating this integral equation of the first kind, we explore the meaning of the surface distribution v. (7), (8) and (9) imply that

$$\left(\frac{\partial \Psi}{\partial t}\right)_i = 0 \ , \tag{11}$$

i.e., that Ψ is constant (Ψ_i) also along the inside of $\mathcal{L}_0$. Green's theorem,

$$\iint (\Psi\Delta\Psi + \Psi_x^2 + \Psi_y^2)\,dx\,dy = \int_{\mathcal{L}_0} \Psi \frac{\partial \Psi}{\partial n}\,ds \ , \tag{12}$$

applied to the inside of $\mathcal{L}_0$ gives

$$\iint (\Psi_x^2 + \Psi_y^2)\,dx\,dy = \Psi_i \int_{\mathcal{L}_0} \frac{\partial \Psi}{\partial n}\,ds = 0 \ ,$$

i.e., inside $\mathcal{L}_0$ the velocity field vanishes identically,

$$\Psi_x = \Psi_y = 0 \ . \tag{13}$$

Therefore

$$\left(\frac{\partial \Psi}{\partial n}\right)_i = 0 \tag{14}$$

which combined with (5) and (6) gives:

$$v = -\left(\frac{\partial \Psi}{\partial n}\right)_o . \tag{15}$$

This means that, by (2) that v represents the magnitude of the flow velocity around $\mathcal{L}_0$ and, from Figure 3, that v is positive (negative) for flow in the counterclockwise (clockwise) direction. The integral equation (10) is a special case ($t = \infty$) of Isay's work [11] which is primarily concerned with a cascade of airfoils, but not recognizing the significance of v as shown in (15).

The integral equation of the second kind that satisfies requirement III is not found as immediately as in the preceding case. One requires that

$$\left(\frac{\partial \Psi}{\partial n}\right)_i = 0 , \tag{16}$$

which leads, by (4) and (6) to the following integral equation of the second kind:

$$v + \frac{1}{\pi} \frac{\partial}{\partial n} \int_{\mathcal{L}_0} v \ln \frac{1}{r} \, ds = -2v_\infty \frac{\partial}{\partial n} (y \cos \alpha - x \sin \alpha) . \tag{17}$$

Again, applying Green's theorem (12) to the inside of $\mathcal{L}_0$, furnishes, on the basis of (16), the result (13) for the velocity field inside $\mathcal{L}_0$. As a result, also

$$\left(\frac{\partial \Psi}{\partial t}\right)_i = 0 \tag{18}$$

and because of (7) and (8), also

$$\left(\frac{\partial \Psi}{\partial t}\right)_0 = 0 \ , \tag{19}$$

i.e., it is established that Ψ is constant along the outside edge of $\mathcal{L}_0$ in accordance with requirement III. The surface distribution v represents the velocity of the flow around $\mathcal{L}_0$ as in the previous example because (5) and (6) again imply (15) in the light of (16). This is a simplified derivation of the integral equation (17) for the velocity distribution v, which was first established by Prager [7].

4. THE PARAMETRIC REPRESENTATION OF $\mathcal{L}_0$

Let the contour $\mathcal{L}_0$ be represented parametrically by

$$x = x(\phi), \qquad y = y(\phi), \qquad 0 \leq \phi \leq 2\pi, \tag{20}$$

with ϕ increasing in the counterclockwise direction. The functions $x(\phi)$ and $y(\phi)$ have periods of 2π and are in accordance with Section 3, supposed to be four times continuously differentiable. Furthermore, in order that one may define a tangential vector at each point on the contour in accordance with Section 3, the subsidiary condition (in addition to (20))

$$[\dot{x}(\phi)]^2 + [\dot{y}(\phi)]^2 \neq 0 \tag{21}$$

is also imposed. With this condition it will be impossible to have cusps on the contour, as was possible with (20) and mere regularity requirements. Finally, to make the following derivation easier, the auxiliary variable $\gamma(\phi)$ will be introduced through the relation

$$v(\phi) = \frac{\gamma(\phi)}{\sqrt{[\dot{x}(\phi)]^2 + [\dot{y}(\phi)]^2}} . \tag{22}$$

The integral equation of the first kind (10) may be put in the following form, where x, y (i.e., ϕ) denotes a fixed point, and ξ, η (i.e., ψ) a variable point on $\mathcal{L}_0$, and $\vec{t}$ is a tangent vector:

$$\begin{aligned} &- \frac{1}{\pi} \frac{\partial}{\partial t} \int_{\mathcal{L}_0} v(\xi, \eta) \ln \frac{1}{r} \, ds \\ &= \frac{1}{2\pi} \frac{\partial}{\partial t} \int_{\mathcal{L}_0} v(\xi, \eta) \ln[(x - \xi)^2 + (y - \eta)^2] \, ds \\ &= \frac{1}{\pi} \int_{\mathcal{L}_0} v(\xi, \eta) \frac{(x - \xi)t_x(x, y) + (y - \eta)t_y(x, y)}{(x - \xi)^2 + (y - \eta)^2} \, ds; \end{aligned}$$

In the light of (22), (10) now becomes

$$\begin{aligned} &- \frac{1}{2\pi} \int_0^{2\pi} \gamma(\psi) \cot \frac{\psi - \phi}{2} \, d\psi + \frac{1}{2\pi} \int_0^{2\pi} H(\phi, \psi) \gamma(\psi) \, d\psi \\ &= 2v_\infty(\dot{y}(\phi) \cos \alpha - \dot{x}(\phi) \sin \alpha) \end{aligned} \tag{23}$$

where

$$\begin{aligned} H(\phi, \psi) = 2 &\frac{[x(\phi) - x(\psi)]\dot{x}(\phi) + [y(\phi) - y(\psi)]\dot{y}(\phi)}{[x(\phi) - x(\psi)]^2 + [y(\phi) - y(\psi)]^2} \\ &- \cot \frac{\phi - \psi}{2} . \end{aligned} \tag{24}$$

Since

$$\lim_{\psi \to \phi} H(\phi, \psi) = \frac{\dot{x}(\phi)\ddot{x}(\phi) + \dot{y}(\phi)\ddot{y}(\phi)}{[\dot{x}(\phi)]^2 + [\dot{y}(\phi)]^2} , \tag{25}$$

$H(\phi, \psi)$ is a continuous kernel everywhere.

Correspondingly, one may modify the integral equation of the second

kind (17), using the parametric representation for $\mathcal{L}_0$ as follows:

$$\frac{1}{\pi}\frac{\partial}{\partial n}\int_{\mathcal{L}_0} v(\xi, \eta)\, \ln\frac{1}{r}\, ds$$

$$= -\frac{1}{2\pi}\frac{\partial}{\partial n}\int_{\mathcal{L}_0} v(\xi, \eta)\, \ln[(x-\xi)^2 + (y-\eta)^2]\, ds$$

$$= -\frac{1}{\pi}\int_{\mathcal{L}_0} v(\xi, \eta)\, \frac{(x-\xi)n_x(x, y) + (y-\eta)n_y(x, y)}{(x-\xi)^2 + (y-\eta)^2}\, ds\ .$$

Because $\vec{n}$ represents the outside unit normal and ϕ increases in the counterclockwise direction,

$$\vec{n} = \frac{1}{\sqrt{[\dot{x}(\phi)]^2 + [\dot{y}(\phi)]^2}} \begin{pmatrix} \dot{y}(\phi) \\ -\dot{x}(\phi) \end{pmatrix}\ . \tag{26}$$

Using (22) and (26), the integral equation (17) takes the following form:

$$\gamma(\phi) - \frac{1}{2\pi}\int_0^{2\pi} K(\phi, \psi)\, \gamma(\psi)\, d\psi = 2v_\infty[\dot{x}(\phi)\cos\alpha + \dot{y}(\phi)\sin\alpha] \tag{27}$$

with

$$K(\phi, \psi) = 2\,\frac{[x(\phi) - x(\psi)]\dot{y}(\phi) - [y(\phi) - y(\psi)]\dot{x}(\phi)}{[x(\phi) - x(\psi)]^2 + [y(\phi) - y(\psi)]^2}\ . \tag{28}$$

Since

$$\lim_{\psi\to\phi} K(\phi, \psi) = \frac{\dot{x}(\phi)\ddot{y}(\phi) - \dot{y}(\phi)\ddot{x}(\phi)}{[\dot{x}(\phi)]^2 + [\dot{y}(\phi)]^2} \tag{29}$$

$K(\phi, \psi)$ is an everywhere continuous kernel. The integral equation (27) arises in Fredholm's treatment of the Neuman problem in potential theory [1; 2] in the form:

$$f(\phi) - \frac{\lambda}{\pi} \int_0^{2\pi} f(\psi) \frac{\partial}{\partial \phi} \arctan \frac{y(\phi) - y(\psi)}{x(\phi) - x(\psi)} \, d\psi = g(\phi) \tag{30}$$

The transpose of equation (30) (replacing $\partial/\partial\phi$ by $\partial/\partial\psi$) was likewise considered by Fredholm for the solution of Dirichlet's problem, and was the starting point of Fredholm's theory of integral equations of the second kind [1].

5. EXISTENCE AND MULTIPLICITY OF THE SOLUTION OF THE INTEGRAL EQUATION OF THE SECOND KIND

In order to decide about the solubility of the integral equation (27) one must investigate, according to the Fredholm theory, the existence of nontrivial solutions of the associated transposed homogeneous integral equation:

$$\tilde{\gamma}(\phi) - \frac{1}{2\pi} \int_0^{2\pi} K(\psi, \phi) \, \tilde{\gamma}(\psi) \, d\psi = 0 \tag{31}$$

We now maintain that

$$\tilde{\gamma}(\phi) = \text{constant} \neq 0 \tag{32}$$

is a nontrivial solution of (31). To prove it, we write

$$\frac{1}{2\pi} \int_0^{2\pi} K(\phi, \psi) \, d\phi = \frac{1}{\pi} \left[\arctan \frac{y(\phi) - y(\psi)}{x(\phi) - x(\psi)} \right]_0^{2\pi}$$

As shown in Figure 4,

$$\tau = \arctan \frac{y(\phi) - y(\psi)}{x(\phi) - x(\psi)}$$

runs through all values from a certain τ_0 to $\tau_0 + \pi$ as ϕ increases from 0 to 2π; each value is assumed at least once. Thereby one obtains the relation

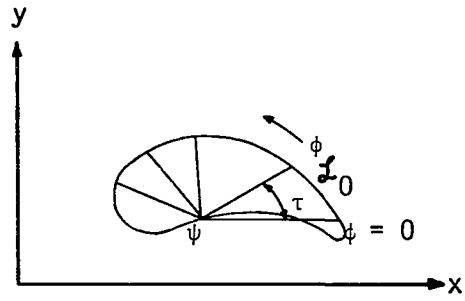

Figure 4

$$\frac{1}{2\pi}\int_0^{2\pi} K(\phi, \psi)\, d\phi = 1 \,, \tag{33}$$

which has already been used by Fredholm [2]. By interchanging ϕ and ψ in (33), one can see that (32) is a nontrivial solution of (31). There we establish the existence of a nontrivial solution $\gamma^*(\phi)$ of (27), when $v_\infty = 0$, which we recognize as the pure circulation flow around the profile. Since it is known from the theory of conformal mapping, that no two linearly independent circulation flows exist it follows, conversely, that the homogeneous equation associated with (27) has not more than one linearly independent solution. Hence we have the degenerate case with a single eigenvalue. The general solution for (27) may be written, therefore, as

$$\gamma(\phi) = \gamma^{**}(\phi) + c\gamma^*(\phi) \,. \tag{34}$$

Here $\gamma^{**}(\phi)$ is the particular solution of the inhomogeneous equation (27).

6. TRANSFORMATION OF THE INTEGRAL EQUATION OF THE FIRST KIND TO AN EQUATION OF THE SECOND KIND, AND THE SOLUBILITY OF THE LATTER

Let $f(\phi)$ be a continuously differentiable function, defined over

$0 \leq \phi \leq 2\pi$, with a period of 2π.

One calls the function,

$$g(\phi) = \frac{1}{2\pi} \int_0^{2\pi} f(\psi) \cot \frac{\psi - \phi}{2} \, d\psi \tag{35}$$

the harmonic conjugate function ("cotangent integral") of $f(\phi)$. (Cauchy principal value is understood.) It results from the Fourier development of $f(\phi)$, by ignoring the constant term and replacing $\cos \nu\phi$ by $-\sin \nu\phi$ and $\sin \nu\phi$ by $\cos \nu\phi$, $\nu = 1, 2, \ldots$. Passing, once more, from $g(\phi)$ to its harmonic conjugate, one obtains:

$$\frac{1}{2\pi} \int_0^{2\pi} g(\psi) \cot \frac{\psi - \phi}{2} \, d\psi = -f(\phi) + \frac{1}{2\pi} \int_0^{2\pi} f(\psi) \, d\psi \, . \tag{36}$$

We now apply the cotangent integral operator to the integral equation of the first kind (23) and obtain the following integral equation of the second kind:

$$\gamma(\phi) - \frac{1}{2\pi} \int_0^{2\pi} L(\phi, \psi) \, \gamma(\psi) \, d\psi$$

$$= \frac{V_\infty}{\pi} \int_0^{2\pi} [\dot{y}(\psi) \cos \alpha - \dot{x}(\psi) \sin \alpha] \cot \frac{\psi - \phi}{2} \, d\psi \tag{37}$$

where

$$L(\phi, \psi) = 1 - \frac{1}{2\pi} \int_0^{2\pi} H(\chi, \psi) \cot \frac{\chi - \phi}{2} \, d\chi \tag{38}$$

is an everywhere continuous kernel. But the integral over a conjugate harmonic function vanishes because of the missing constant term in the Fourier development; thus (38) leads to:

$$\frac{1}{2\pi} \int_0^{2\pi} L(\phi, \psi) \, d\phi = 1 \, . \tag{39}$$

As in Section 5, it is now established that the general solution of (37)

is in the form of (34).

7. DERIVATION OF THE INTEGRAL EQUATION FOR A CASCADE OF AIRFOILS

Similarly as above, two integral equations of the second kind will be derived for the velocity distribution on a cascade of thick airfoils (Figure 1) corresponding to (27) and (37). We thus expect two equations of the form

$$\gamma(\phi) - \frac{1}{2\pi}\int_0^{2\pi} K(\phi, \psi; t)\,\gamma(\psi)\,d\psi = 2v_\infty[\dot{x}(\phi)\cos\alpha + \dot{y}(\phi)\sin\alpha] \tag{40}$$

and

$$\gamma(\phi) - \frac{1}{2\pi}\int_0^{2\pi} L(\phi, \psi; t)\,\gamma(\psi)\,d\psi = \frac{v_\infty}{\pi}\int_0^{2\pi} [\dot{y}(\psi)\cos\alpha - \dot{x}(\psi)\sin\alpha]\cot\frac{\psi - \phi}{2}\,d\psi \tag{41}$$

which for $t \to \infty$ will reduce to (27) and (37), respectively. The quantities v_∞ and α still to be clarified, since infinity with respect to the cascade is not simply related to the "outside" of the contours $\mathcal{L}_0$, $\mathcal{L}_1$, $\mathcal{L}_{-1}$, ... Because of this we relinquish for the time being requirement II of Section 3 and treat v_∞ and α merely as free parameters, whereas we shall retain requirements I and III for all contours $\mathcal{L}_0$, $\mathcal{L}_1$, $\mathcal{L}_{-1}$, ... Then the stream function expression which satisfies requirement I is given by

$$\Psi(x, y; t) = v_\infty(y\cos\alpha - x\sin\alpha) + \frac{1}{2\pi}\int_{\mathcal{L}_0} v\,\ln\frac{1}{\sqrt{\cosh\frac{2\pi}{t}(x - \xi) - \cos\frac{2\pi}{t}(y - \eta)}}\,ds + \text{constant} . \tag{42}$$

This expression and formula (4) have already been found by Goldstein and Jerison [10]. Furthermore, it can be seen from (42) that

$$\left.\begin{aligned} \Psi_x(x, y; t) &= \Psi_x(x, y + kt; t) \\ \Psi_y(x, y; t) &= \Psi_y(x, y + kt; t) \end{aligned}\right\}, \quad k = \pm 1, \pm 2, \pm 3, \ldots , \tag{43}$$

so that if requirement III is satisfied for $\mathcal{L}_0$ alone, then it will be satisfied for all of $\mathcal{L}_1$, $\mathcal{L}_{-1}$, ... as well. Therefore, we can confine the investigation to the conditions at $\mathcal{L}_0$. It will be shown next that relations (5) to (8) are valid also for (42). For this purpose, we will investigate the expression

$$F(x, y; t) = \frac{1}{4\pi} \int_{\mathcal{L}_0} v \ln \left\{ 2 \frac{\cosh \frac{2\pi}{t}(x - \xi) - \cos \frac{2\pi}{t}(y - \eta)}{[\frac{2\pi}{t}(x - \xi)]^2 + [\frac{2\pi}{t}(y - \eta)]^2} \right\} ds . \tag{44}$$

First, one can establish that, for fixed t, F(x, y; t) is an analytic function outside of $\mathcal{L}_0$, $\mathcal{L}_1$, $\mathcal{L}_{-1}$, ... This is equally valid for the inside regions of $\mathcal{L}_0$, $\mathcal{L}_1$, $\mathcal{L}_{-1}$, ... Next we show that F(x, y; t) is analytic on $\mathcal{L}_0$ itself (not for $\mathcal{L}_1$, $\mathcal{L}_{-1}$, ...). For this purpose we set

$$\frac{2\pi}{t}(x - \xi) = X \tag{45}$$

$$\frac{2\pi}{t}(y - \eta) = Y \tag{46}$$

and expand the argument for the logarithm in (44) as follows:

$$2\,\frac{\cosh X - \cos Y}{X^2 + Y^2}$$

$$= 2\,\frac{\sum_{\nu=0}^{\infty} \frac{X^{2\nu+2}}{(2\nu+2)!} - \sum_{\nu=0}^{\infty} (-1)^{\nu+1} \frac{Y^{2\nu+2}}{(2\nu+2)!}}{X^2 + Y^2}$$

$$= 2 \sum_{\nu=0}^{\infty} \frac{1}{(2\nu+2)!} \frac{(X^2)^{\nu+1} - (-Y^2)^{\nu+1}}{X^2 - (-Y^2)}$$

$$= 2 \sum_{\nu=0}^{\infty} \frac{1}{(2\nu+2)!} \sum_{\mu=0}^{\nu} (X^2)^{\nu-\mu} (-Y^2)^{\mu} .$$

To show that the series converges for all values of X and Y we let (with M equal to a real positive number)

$$|X| \leq M, \qquad |Y| < M .$$

The estimate

$$\left| 2\,\frac{\cosh X - \cos Y}{X^2 + Y^2} \right| \leq 2 \sum_{\nu=0}^{\infty} \frac{1}{(2\nu+2)!} \cdot (\nu+1) M^{2\nu} = \frac{\sinh M}{M} .$$

is thereby established. Thus

$$2\,\frac{\cosh X - \cos Y}{X^2 + Y^2} = 1 + \frac{X^2 - Y^2}{12} + \frac{X^4 - X^2Y^2 + Y^4}{360} + \cdots \qquad (47)$$

is convergent for all values of X and Y and hence is an entire function in both variables, X and Y. Therefore, the series

$$\ln \left\{ 2\,\frac{\cosh X - \cos Y}{X^2 - Y^2} \right\} = \frac{X^2 - Y^2}{12} - \frac{X^4 - 6X^2Y^2 + Y^4}{1440} + \cdots \qquad (48)$$

(which follows from (47)) also converges in a finite region from X = 0, Y = 0, and therefore represents there an analytic function in X and Y. Finally, the integrand of (44), with fixed ξ, η and t, is also analytic for all values of x and y on $\mathcal{I}_0$ (including the inside and outside of $\mathcal{I}_0$,

excepting $\mathcal{L}_1$, $\mathcal{L}_{-1}$, ...). As a result, $F(x, y; t)$ experiences no discontinuities as one crosses $\mathcal{L}_0$. Finally, since the form (42) for $\Psi(x, y; t)$ differs from (4) for $\Psi(x, y)$ only by the expression,

$$-F(x, y; t) + \text{constant},$$

equations (5) to (8) are seen to be valid also for expression (42). One can thus transfer the reasoning of Sections 3 and 4, without additional considerations, to cascades. Also, the requirement III can be thought of as being fulfilled by the corresponding integral equations (40) and (41). As stated before, the corresponding flow conditions for $\mathcal{L}_1$, $\mathcal{L}_{-1}$, ... are also automatically satisfied.

Now, all that remains is the clarification of the significance of v_∞, α and of the kernels $K(\phi, \psi; t)$ and $L(\phi, \psi; t)$ which appear in equations (40) and (41). It follows from (42) that:

$$\left.\begin{aligned} \lim_{x\to-\infty} \Psi_x(x, y; t) &= -v_\infty \sin\alpha + \frac{1}{2t}\int_{\mathcal{L}_0} v\, ds \\ \lim_{x\to+\infty} \Psi_x(x, y; t) &= -v_\infty \sin\alpha - \frac{1}{2t}\int_{\mathcal{L}_0} v\, ds \\ \lim_{x\to\pm\infty} \Psi_y(x, y; t) &= v_\infty \cos\alpha \end{aligned}\right\} \tag{49}$$

with

$$\Gamma = \int_{\mathcal{L}_0} v\, ds = \int_0^{2\pi} \gamma(\phi)\, d\phi \tag{50}$$

representing the circulation around each cascade profile, one obtains from (1):

$$\left.\begin{aligned} w_{x,-\infty} &= w_{x,+\infty} = v_\infty \cos\alpha \\ w_{y,-\infty} &= v_\infty \sin\alpha - \frac{\Gamma}{2t} \\ w_{y,+\infty} &= v_\infty \sin\alpha + \frac{\Gamma}{2t}\,. \end{aligned}\right\} \tag{51}$$

$w_{x,\infty} = v_\infty \cos\alpha$ and $w_{y,\infty} = v_\infty \sin\alpha$ are now recognized as components of the so-called "transport flow velocity," $\vec{w}_\infty$ (vector average of the upstream velocity $\vec{w}_{-\infty}$ and downstream velocity $\vec{w}_{+\infty}$) shown in Figure 5. Furthermore,

$$w_{y,+\infty} - w_{y,-\infty} = \frac{\Gamma}{t} \tag{52}$$

is the characteristic "deflection" caused by the cascade.

To obtain the forms of the kernels $K(\phi, \psi; t)$ and $L(\phi, \psi; t)$, we proceed as in Section 4 (being careful not to confuse $\partial/\partial t$ and the pitch t), and obtain an integral equation of the first kind:

$$-\frac{1}{\pi}\frac{\partial}{\partial t}\int_{\mathcal{L}_0} v(\xi, \eta)\, \ln \frac{1}{\sqrt{\cosh\frac{2\pi}{t}(x-\xi) - \cos\frac{2\pi}{t}(y-\eta)}}\, ds$$

$$= \frac{1}{t}\int_{\mathcal{L}_0} v(\xi, \eta)\, \frac{[\sinh\frac{2\pi}{t}(x-\xi)]t_x(x, y) + [\sin\frac{2\pi}{t}(y-\eta)]t_y(x, y)}{\cosh\frac{2\pi}{t}(x-\xi) - \cos\frac{2\pi}{t}(y-\eta)}\, ds$$

This differs from (23) only by the kernel

$$H(\phi, \psi; t) = \frac{2\pi}{t}\, \frac{[\sinh\frac{2\pi}{t}(x-\xi)]\dot{x}(\phi) + [\sin\frac{2\pi}{t}(y-\eta)]\dot{y}(\phi)}{\cosh\frac{2\pi}{t}(x-\xi) - \cos\frac{2\pi}{t}(y-\eta)}$$

$$- \cot\frac{\phi - \psi}{2} \tag{53}$$

and in this form was the basis of Isay's work. As can be easily shown,

the limiting value (25) for $H(\phi, \psi; t)$ is still valid. Correspondingly, one establishes an integral equation of the second kind analogous to (27):

$$\frac{1}{\pi}\frac{\partial}{\partial n}\int_{\mathcal{L}_0} v(\xi, \eta)\, \ln \frac{1}{\sqrt{\cosh \frac{2\pi}{t}(x - \xi) - \cos \frac{2\pi}{t}(y - \eta)}}\, ds$$

$$= -\frac{1}{t}\int_{\mathcal{L}_0} v(\xi, \eta)\, \frac{[\sinh \frac{2\pi}{t}(x - \xi)]n_x + [\sin \frac{2\pi}{t}(y - \eta)]n_y}{\cosh \frac{2\pi}{t}(x - \xi) - \cos \frac{2\pi}{t}(y - \eta)}\, ds$$

with the kernel:

$$K(\phi, \psi; t) = \frac{2\pi}{t}\, \frac{[\sinh \frac{2\pi}{t}(x - \xi)]\dot{y}(\phi) - [\sin \frac{2\pi}{t}(\phi - \eta)]\dot{x}(\phi)}{\cosh \frac{2\pi}{t}(x - \xi) - \cos \frac{2\pi}{t}(y - \eta)} \tag{54}$$

Also $K(\phi, \psi; t)$ retains its limiting value. Finally the kernel $L(\phi, \psi; t)$ corresponding to Section 6 assumes the expression:

$$L(\phi, \psi; t) = 1 - \frac{1}{2\pi}\int_0^{2\pi} H(\chi, \psi; t)\, \cot \frac{\chi - \phi}{2}\, d\chi \tag{55}$$

With this, one can handle all the terms in the integral equations (40) and (41) for the treatment of the cascade problem.

8. EXISTENCE AND MULTIPLICITY OF THE SOLUTIONS FOR THE INTEGRAL EQUATIONS OF THE SECOND KIND FOR A CASCADE OF AIRFOILS

One shows that the homogeneous integral equations (40) and (41) possess nontrivial solutions by verifying, as in Sections 5 and 6, that

$$\frac{1}{2\pi}\int_0^{2\pi} K(\phi, \psi; t)\, d\phi = 1 \tag{56}$$

$$\frac{1}{2\pi}\int_0^{2\pi} L(\phi, \psi; t)\, d\phi = 1 . \tag{57}$$

While the proof of (57) follows directly from the definition (55) for $L(\phi, \psi; t)$, the proof of (56) is not obtained as easily. First of all, we define

$$J(\psi; t) = \frac{1}{2\pi}\int_0^{2\pi} K(\phi, \psi; t)\, d\phi \tag{58}$$

which leads, with the aid of (54), to

$$J(\psi; 2t) = \frac{1}{2t}\int_0^{2\pi} \frac{[\sinh \frac{\pi}{t}(x-\xi)]\dot{y}(\phi) - [\sin \frac{\pi}{t}(y-\eta)]\dot{x}(\phi)}{\cosh \frac{\pi}{t}(x-\xi) - \cos \frac{\pi}{t}(y-\eta)}\, d\phi$$

$$= \frac{1}{2t}\int_0^{2\pi} \frac{[\sinh \frac{\pi}{t}(x-\xi)\cosh \frac{\pi}{t}(x-\xi)]\dot{y}(\phi)}{\cosh^2 \frac{\pi}{t}(x-\xi) - \cos^2 \frac{\pi}{t}(y-\eta)}$$

$$- \frac{[\sin \frac{\pi}{t}(y-\eta)\cos \frac{\pi}{t}(y-\eta)]\dot{x}(\phi)}{\cosh^2 \frac{\pi}{t}(x-\xi) - \cos^2 \frac{\pi}{t}(y-\eta)}\, d\phi$$

$$+ \frac{1}{2\pi}\int_0^{2\pi} \frac{[\sinh \frac{\pi}{t}(x-\xi)\cos \frac{\pi}{t}(y-\eta)]\dot{y}(\phi)}{\cosh^2 \frac{\pi}{t}(x-\xi) - \cos^2 \frac{\pi}{t}(y-\eta)}$$

$$- \frac{[\sin \frac{\pi}{t}(y-\eta)\cosh \frac{\pi}{t}(x-\xi)]\dot{x}(\phi)}{\cosh^2 \frac{\pi}{t}(x-\eta) - \cos^2 \frac{\pi}{t}(y-\eta)}\, d\phi$$

$$= \frac{1}{2t}\int_0^{2\pi} \frac{[\sinh \frac{2\pi}{t}(x-\xi)]\dot{y}(\phi) - [\sin \frac{2\pi}{t}(y-\eta)]\dot{x}(\phi)}{[1+\cosh \frac{2\pi}{t}(x-\xi)] - [1+\cos \frac{2\pi}{t}(y-\eta)]}\, d\phi$$

$$+ \frac{1}{2\pi}\left[\arctan \frac{\sin \frac{\pi}{t}(y-\eta)}{\sinh \frac{\pi}{t}(x-\xi)}\right]_0^{2\pi} .$$

Now, by arguments similar to those pertaining to Figure 4, one obtains, on the basis of (54) and (58):

$$J(\psi;\ 2t) = \frac{1}{2}\, J(\psi;\ t) + \frac{1}{2}\ . \tag{59}$$

Furthermore,

$$J(\psi;\ 4t) = \frac{1}{4}\, J(\psi;\ t) + \frac{1}{4} + \frac{1}{2}$$

$$J(\psi;\ 8t) = \frac{1}{8}\, J(\psi;\ t) + \frac{1}{8} + \frac{1}{4} + \frac{1}{2}$$

$$\vdots$$

and

$$J(\psi;\ 2^{\nu}t) = 2^{-\nu}J(\psi;\ t) + 2^{-\nu}(1 + 2 + 2^2 + \cdots + 2^{\nu-1})$$

$$= 1 + 2^{\nu}[J(\psi;\ 2^{\nu}t) - 1],\quad \nu = 0,\ 1,\ 2,\ \ldots \tag{60}$$

on noting

$$1 + 2 + 2^2 + \cdots + 2^{\nu-1} = 2^{\nu} - 1\ .$$

We now set

$$\frac{2\pi}{t} = z \tag{61}$$

and investigate the analyticity of (54) with respect to z (in the neighborhood of $z = 0$) in the form

$$K(\phi,\ \psi;\ \frac{2\pi}{z}) = z\,\frac{[\sinh z(x - \xi)]\dot{y}(\phi) - [\sin z(\phi - \eta)]\dot{x}(\phi)}{\cosh z(x - \xi) - \cos z(y - \eta)} \tag{62}$$

for fixed ϕ and ψ.

Expanding numerator and denominator of the last expression in power of z one obtains:

$$K(\phi,\ \psi;\ \frac{2\pi}{t})$$

$$= \frac{\left(\sum_{\nu=0}^{\infty} \frac{(x-\xi)^{2\nu+1}}{(2\nu+1)!}\, z^{2\nu}\right)\dot{y}(\phi) - \left(\sum_{\nu=0}^{\infty} (-1)^{\nu}\, \frac{(y-\eta)^{2\nu+1}}{(2\nu+1)!}\, z^{2\nu}\right)\dot{x}(\phi)}{\sum_{\nu=0}^{\infty} \frac{(x-\xi)^{2\nu+2}}{(2\nu+2)!}\, z^{2\nu} - \sum_{\nu=0}^{\infty} (-1)^{\nu+1}\, \frac{(y-\eta)^{2\nu+2}}{(2\nu+2)!}\, z^{2\nu}} \tag{63}$$

The constant term in the denominator does not vanish when

$$\psi \neq \phi + 2k\pi \ , \qquad k = 0, \pm 1, \pm 2, \ \ldots \ .$$

Thus there exists a neighborhood of $z = 0$ where $K(\phi, \psi; \frac{2\pi}{z})$ is analytic, and may be represented by a convergent power series.

$$K(\phi, \psi; \tfrac{2\pi}{z}) = 2 \frac{(x - \xi)\dot{y}(\phi) - (y - \eta)\dot{x}(\phi)}{(x - \xi)^2 + (y - \eta)^2} + f_1(\phi, \psi)z^2 + f_2(\phi, \psi)z^4 + \cdots \tag{64}$$

Since the limiting value, as $\psi \to \phi + 2k\pi$ exists on the left side, it must also exist on the right side and must hold for each coefficient of $z^{2\nu}$. In this limit therefore, the dependence on z disappears as seen from (29). Thus $K(\phi, \phi + 2k\pi, \frac{2\pi}{z})$ is a constant and hence analytic. It follows that $K(\phi, \psi; \frac{2\pi}{z})$ is analytic for all values of ϕ, ψ in a certain vicinity of $z = 0$ and admits a power series representation (64).

Because of uniform convergence for fixed ψ and z, we may integrate (64) with respect to ϕ term by term, and obtain on the basis of (33), (58) and (61) the expansion

$$J(\psi; t) = 1 + \frac{F_1(\psi)}{t^2} + \frac{F_2(\psi)}{t^4} + \cdots \tag{65}$$

which converges for sufficiently large t. We select ν for a specific cascade so large that

$$J(\psi; 2^{\nu}t) = 1 + \frac{F_1(\psi)}{2^{2\nu}t^2} + \frac{F_2(\psi)}{2^{4\nu}t^4} + \cdots$$

converges for all values of ψ (such a ν may always be found). Replacement into (60) now gives:

$$J(\psi;\ t) = 1 + \frac{F_1(\psi)}{2^{\nu}t^2} + \frac{F_2(\psi)}{2^{3\nu}t^4} + \cdots$$

which is valid for the chosen ν and all greater values. Using $\nu \to \infty$,

$$J(\psi;\ t) = 1 \tag{66}$$

follows as well as statement (56).

9. NUMERICAL AUXILIARIES

The interpolation formula for a function $f(\phi)$ specified by

$$f_\nu = f(\phi_\nu)\ , \qquad \phi_\nu = \frac{\nu\pi}{N}\ , \qquad \nu = 0,\ \ldots\ ,\ (2N - 1)\ . \tag{67}$$

with periodicity 2π is the trigonometric polynomial

$$f(\phi) = \sum_{\mu=0}^{N} a_\mu \cos \mu\phi + \sum_{\mu=1}^{N-1} b_\mu \sin \mu\phi\ , \tag{68}$$

where

$$\left.\begin{aligned} a_0 &= \frac{1}{2N}\sum_{\nu=0}^{2N-1} f_\nu \\ a_\mu &= \frac{1}{N}\sum_{\nu=0}^{2N-1} f_\nu \cos \mu\phi_\nu\ , \qquad \mu = 1,\ \ldots\ ,\ (N - 1) \\ a_N &= \frac{1}{2N}\sum_{\nu=0}^{2N-1} (-1)^\nu f_\nu \\ b_\mu &= \frac{1}{N}\sum_{\nu=0}^{2N-1} f_\nu \sin \mu\phi_\nu\ , \qquad \mu = 1,\ \ldots\ ,\ (N - 1) \end{aligned}\right\} \tag{69}$$

The following formulas result from this representation.

Integration:

$$\frac{1}{2\pi}\int_0^{2\pi} f(\phi)\ d\phi = \frac{1}{2N}\sum_{\nu=0}^{2N-1} f_\nu\ ; \tag{70}$$

Cotangent Integral:

$$\frac{1}{2\pi}\int_0^{2\pi} f(\psi)\,\cot\frac{\psi-\phi_\mu}{2}\,d\psi = \sum_{\nu=1}^{2N-1} A_\nu f_{\mu+\nu} \tag{71}$$

with

$$A_\nu = \frac{1-(-1)^\nu}{2N}\cot\frac{\phi_\nu}{2}\ ; \qquad \nu = 1, \ldots, (2N-1)\ ; \tag{72}$$

Differentiation:

$$\dot{f}(\phi_\mu) = \dot{f}_\mu = \sum_{\nu=1}^{2N-1} B_\nu f_{\mu+\nu} \tag{73}$$

with

$$B_\nu = \frac{(-1)^{\nu-1}}{2}\cot\frac{\phi_\nu}{2}\ , \qquad \nu = 1, \ldots, (2N-1)$$

10. PRACTICAL CALCULATION PROCEDURE

Using the above, equations (40) and (41) are converted to the following systems of linear equations:

$$\gamma_\mu - \frac{1}{2N}\sum_{\nu=0}^{2N-1} K_{\mu\nu}\gamma_\nu = 2v_\infty[\dot{x}_\mu\cos\alpha + \dot{y}_\mu\sin\alpha] \tag{74a}$$

$$\gamma_\mu - \frac{1}{2N}\sum_{\nu=0}^{2N-1} L_{\mu\nu}\gamma_\nu = \frac{v_\infty}{\pi}\int_0^{2\pi}[\dot{y}(\psi)\cos\alpha - \dot{x}(\psi)\sin\alpha]\cot\frac{\psi-\phi_\mu}{2}\,d\psi$$

$$\mu = 0, \ldots, (2N-1)\ . \tag{74b}$$

Summing up all the above equations for both systems (74), it follows from previous work that (74a) is nearly linearly dependent, while in (74b) the linear dependence is exact. Thus, one can omit any equation in the second system (e.g., the $\mu = 0$ equation) while the first system

should be solved in a least square sense. To accomplish this (74a) is rendered, on the basis of (56), which is written as

$$\frac{1}{2N}\sum_{\mu=0}^{2N-1}\left\{\gamma_\mu - \frac{1}{2N}\sum_{\nu=0}^{2N-1} K_{\mu\nu}\gamma_\nu\right\} = \frac{1}{2N}\sum_{\nu=0}^{2N-1}\left(1 - \frac{1}{2N}\sum_{\mu=0}^{2N-1} K_{\mu\nu}\right)\gamma_\nu = 0 \ , \tag{75}$$

linearly dependent. Again any equation, say, the $\mu = 0$ equation, may be omitted. Therefore, we have a system of $(2N - 1)$ equations for $2N$ unknowns $\gamma_0, \gamma_1, \ldots, \gamma_{2N-1}$. The $(2N)^{th}$ equation is obtained from relation (50) for the total circulation, numerically represented by:

$$\frac{1}{2N}\sum_{\nu=0}^{2N-1} \gamma_\nu = \frac{\Gamma}{2\pi} \tag{76}$$

The totality of solutions can be obtained by the superposition of all possible solutions. It suffices to solve (74) for three inhomogeneous sides, a_μ, b_μ and c_μ, where a_μ and b_μ correspond to the perpendicular flow ($\alpha = 0$) and parallel flow ($\alpha = \pi/2$), respectively, to the cascade in the absence of circulation ($\Gamma = 0$). The third inhomogeneous side c_μ specifies a free circulation flow with no incoming flow ($v_\infty = 0$). Thus, we have the following:

$$a_\mu = \begin{cases} 2v_\infty \dot{x}_\mu \text{ and } \dfrac{v_\infty}{\pi}\displaystyle\int_0^{2\pi} \dot{y}(\psi)\cot\frac{\psi - \phi_\mu}{2}\,d\psi \ , & \\ & \mu = 1, \ldots, (2N-1), \\ 0 & \mu = 2N \ , \end{cases} \tag{77}$$

$$b_\mu = \begin{cases} 2v_\infty \dot{y}_\mu \text{ and } -\dfrac{v_\infty}{\pi}\displaystyle\int_0^{2\pi} \dot{x}(\psi)\cot\frac{\psi - \phi_\mu}{2}\,d\psi & \\ & \mu = 1, \ldots, (2N-1), \\ 0 & \mu = 2N \ , \end{cases} \tag{78}$$

$$c_\mu = \begin{cases} 0 & \mu = 1, \ldots, (2N-1), \\ \frac{\Gamma}{2\pi} & \mu = 2N . \end{cases} \tag{79}$$

In the numerical calculations it is desirable to make x_μ and y_μ dimensionless, set $v_\infty = 1$ and $\Gamma = 2\pi$. In superimposing free circulation one must take into account, for cascades, the upstream and downstream flow modifications according to (51). Noting (22), we denote the three above solutions $v^{(1)}(\phi)$, $v^{(2)}(\phi)$ and $v^{(3)}(\phi)$ and refer to them as the fundamental solutions. Thus

$$\frac{v_\nu}{v_{-\infty}} = a v_\nu^{(1)} + b v_\nu^{(2)} + c v_\nu^{(3)} , \quad \nu = 0, \ldots, (2N-1) , \tag{80}$$

where

$$\begin{aligned} a &= \cos \alpha_{-\infty} \\ b &= \frac{1}{2} (\cos \alpha_{-\infty} \tan \alpha_{+\infty} + \sin \alpha_{-\infty}) \\ c &= \frac{t}{2\pi} (\cos \alpha_{-\infty} \tan \alpha_{+\infty} - \sin \alpha_{-\infty}) \end{aligned} \tag{81}$$

represents the solution with $\alpha_{-\infty}$ equal to the upstream flow angle and $\alpha_{+\infty}$ equal to the downstream flow angle (Figure 5). The accompanying pressure distribution is given by:

$$c_{p,\nu} = \frac{p_\nu - p_{-\infty}}{\frac{\rho}{2} v_{-\infty}^2} = 1 - (v_\nu / v_{-\infty})^2 , \quad \nu = 0, \ldots, (2N-1) , \tag{82}$$

while the expression for the total circulation from (52) and (81)--see Figure 5--is given by

$$\frac{\Gamma}{v_{-\infty}} = t(\cos \alpha_{-\infty} \tan \alpha_{+\infty} - \sin \alpha_{-\infty}) = 2\pi c . \tag{83}$$

It is to be noted that a and b are dimensionless constants whereas c has the dimension of length.

In the following, the solutions of the integral equations (27) and (40) will be referred to as procedure A, while the solutions of the integral equations (37) and (41) will be referred to as procedure B.

11. EXAMPLE FOR 2N = 24 CONTOUR POINTS

First of all, we shall compare the results of the foregoing analysis with the known solution for a single ellipse of thickness ratio $0 < \varepsilon < 1$ (cf. introduction of this report). The parametric representation is given by:

$$\left.\begin{aligned} x(\phi) &= \cos\phi \\ y(\phi) &= \varepsilon \sin\phi \end{aligned}\right\} \quad 0 \leq \phi \leq 2\pi \tag{84}$$

At an angle of attack α_s, the fundamental solutions are, as obtained by the methods of conformal mapping:

$$\left.\begin{aligned} v^{(1)}(\phi) &= -\frac{(1+\varepsilon)\sin(\phi-\alpha_s)}{\sqrt{\sin^2\phi + \varepsilon^2\cos^2\phi}} \\ v^{(2)}(\phi) &= \frac{(1+\varepsilon)\cos(\phi-\alpha_s)}{\sqrt{\sin^2\phi + \varepsilon^2\cos\phi}} \\ v^{(3)}(\phi) &= \frac{1}{\sqrt{\sin^2\phi + \varepsilon^2\cos\phi}} \end{aligned}\right\} , \; 0 \leq \phi \leq 2\pi \; ; \tag{85}$$

(See Table 1 and Figure 6 deleting one of the two ellipses.) The results are shown for $\varepsilon = 0.2$ and $\alpha_s = 30°$ in Table 2 (procedure A) and Table 3 (procedure B). These agree throughout to nearly four significant figures with the exact solution (Table 1). The error is thus far below the graphical accuracy. A cascade of these contours, with pitch ratio

t/ℓ, equal to 1.0, will be investigated next (Table 4 and Figures 5 and 6). Since, at the present time, there is no known exact, closed solution to this problem, one must content oneself with the fact that both above independent procedures lead to results which agree to nearly four significant figures.

The pressure distributions for two contours with sharp trailing edges, designated as No. 9 and No. 10, were calculated for various upstream flow conditions and for $t/\ell = 1$ and $\alpha_s = 40°$. The fundamental solutions, calculated by procedures A and B (Tables 6 and 7), show some disagreement near the trailing edge. This is not surprising, since cases with sharp trailing edges were excluded from the beginning, and the large curvature of the given contours make them appear as if they had cusps. However, this does not prevent a good agreement between theory and measurements for contour No. 9 (Figures 9 to 13). The upstream flow angle $\alpha_{-\infty}$ is varied from -15° to 45° in intervals of 15°, while for the downstream flow angle the experimental, nearly constant, $\alpha_{+\infty} = -69.6°$ was chosen. The numerical values for these cases are collected in the following chart:

$\alpha_{-\infty}$	$\alpha_{+\infty}$	a	b	c/t	$\Gamma/\ell v_{-\infty}$	$c_{p,+\infty}$
-15°	- 69.6°	0.9659	-1.4281	-0.3722	-2.3385	-6.6791
0°	- 69.6°	1.0000	-1.3445	-0.4280	-2.6889	-7.2304
15°	- 69.6°	0.9659	-1.1693	-0.4546	-2.8561	-6.6791
30°	- 69.6°	0.8660	-0.9143	-0.4502	-2.8287	-5.1753
45°	- 69.6°	0.7071	-0.5971	-0.4152	-2.6085	-3.1152

For simplicity, contour No. 10 will be investigated next ($t/\ell = 1$, $\alpha_s = 40°$) using procedure B only (Table 8, Figure 8). In order to evaluate the relative merits of contours No. 9 and No. 10 (see Figure 8) we let, for both contours, the stagnation point coincide with the trailing edge ($\phi = 0$ and $\nu = 0$, respectively) and set the upstream flow angle ($\alpha_{-\infty}$) equal zero. For superposition of the fundamental solutions, the following coefficients are required (see formulas (81)):

Contour	$\alpha_{-\infty}$	$\alpha_{+\infty}$	a	b	c/t	$\Gamma/\ell c_{-\infty}$
No. 9	0°	-72.5°	1.0000	-1.5851	-0.5046	-3.1703
No. 10	0°	-70.9°	1.0000	-1.4470	-0.4606	-2.8940

Both resultants are displayed in Figure 14.

Finally, a further contour, designated No. 12, will be investigated (Table 9, Figures 15 and 16). An upstream flow angle $\alpha_{-\infty} = 0$ is assumed and the rear stagnation point will again be placed at the trailing edge ($\phi = 0$ and $\nu = 0$, respectively). The solution is carried out with:

$\alpha_{-\infty}$	$\alpha_{+\infty}$	a	b	c/t	$\Gamma/\ell v_{-\infty}$
0°	-71.3°	1.0000	-1.4762	-0.4699	-2.9523

The theoretical pressure distribution, calculated by procedure B, is shown in Figure 17.

The numerical calculations were carried out on the moderate speed Göttingen G2 computer (approximately 20 operations/sec). The approximate computation time for a single calculation amounted to the following:

Single airfoil with procedure A -- 1 hour 15 minutes

Single airfoil with procedure B -- 1 hour 45 minutes

Cascade of airfoils with procedure A -- 3 hours 15 minutes

Cascade of airfoils with procedure B -- 3 hours 45 minutes

The computer program is so arranged that only the angle of attack, pitch ratio and contour coordinates must be supplied to the machine. The program will then be automatically carried through after the machine is started, and without further input, it will end by automatically outputting the expressions of the contour data, and the desired fundamental solutions.

The author thanks Dr. F. W. Riegels for his encouragement and assistance in this work and Professor Dr. Biermann for providing the G2 computer. The support for this investigation was provided by the "Deutchen Forschungsgemeinshaft."

The theoretical part of this investigation was presented on 5 December 1957 in a Seminar on Instrumental Mathematics at the Max Planck Institute for Physics.

Translated for the National Aeronautics and Space Administration
by R. J. Weetman
Department of Mechanical and Aerospace Engineering
University of Massachusetts
Amherst, Mass. 01003

REFERENCES

[1] I. Fredholm, "On a New Method to Solve Dirichlet's Problem," Öefvers. of Kgl. Vetensk. Ak. Föck. Stockh. 57, No. 1 (1900), pp. 39-46.

[2] I. Fredholm, "On an Integral Equation with an Analytical Kernel," Acta Math. 45 (1924), pp. 11-27.

[3] W. Schmeidler, Integral Equations with Applications in Physics and Engineering, Vol. I, Leipzig, 1950.

[4] R. Courant and D. Hilbert, Methods of Mathematics Physics, Vols. I and II, Berlin, 1931 and 1937, respectively.

[5] A. Korn, Textbook on Potential Theory, Berlin, 1899.

[6] L. Prandtl, Airfoil Theory, Vol. 1, Report of the Imperial Association for Science, Göttingen, Math-Phys. Class 1918, pp. 451-477.

[7] W. Prager, "The Pressure Distribution on Bodies in Plane Potential Flow," Physik. Zeitschr. 29 (1928), pp. 865-869.

[8] E. J. Nyström, "Practical Solution of Linear Integral Equations with Applications to Boundary Value Problems in Potential Theory," Comm. Phys.-Math. Soc. Scient. Fennica 4, No. 15 (1928), pp. 1-25.

[9] H. Föttinger, "The Development of Vectorial Integration to Computer Solutions for Potential and Vortex Problems," Zeitschr. f. Techn. Phys., 1928.

[10] A. W. Goldstein and M. Jerison, "Isolated and Cascade Airfoils with Prescribed Velocity Distributions," NACA Techn. Rep. No. 869 (1957), pp. 201-215.

[11] W. H. Isay, "Comments on the Potential Flow through Axial Cascades," Dissertation, Z. f. Angew. Math. & Mech., 33 (1953), pp. 397-409.

[12] Hütte, The Engineer's Handbook, Vol. 1, 26. Aufl., Berlin, 1936, p. 191.

[13] N. Scholz, Report 52/25, Institute for Flow Mechanics of the Technical University, Braunschweig (1952)(unpublished).

TABLE 1. Coordinates and the exact values of the fundamental solutions for a 20% thick single ellipse at an angle of attack $\alpha_s = 30°$.

ν	x_ν	y_ν	$\dot{s}_\nu$	$v_\nu^{(1)}$	$v_\nu^{(2)}$	$v_\nu^{(3)}$
0	1.0000000	0.0000000	0.20000	3.00000	5.19615	5.00000
1	0.9659258	0.0517638	0.32297	0.96165	3.58894	3.09629
2	0.8660254	0.1000000	0.52915	0.00000	2.26779	1.88982
3	0.7071068	0.1414214	0.72111	-0.43070	1.60740	1.38675
4	0.5000000	0.1732051	0.87178	-0.68825	1.19208	1.14708
5	0.2588190	0.1931852	0.96731	-0.87720	0.87720	1.03379
6	0.0000000	0.2000000	1.00000	-1.03923	0.60000	1.00000
7	-0.2588190	0.1931852	0.96731	-1.19828	0.32108	1.03379
8	-0.5000000	0.1732051	0.87178	-1.37649	0.00000	1.14708
9	-0.7071068	0.1414214	0.72111	-1.60740	-0.43070	1.38675
10	-0.8660254	0.1000000	0.52915	-1.96396	-1.13389	1.88982
11	-0.9659258	0.0517638	0.32297	-2.62729	-2.62729	3.09629
12	-1.0000000	0.0000000	0.20000	-3.00000	-5.19615	5.00000
13	-0.9659258	-0.0517638	0.32297	-0.96165	-3.58894	3.09629
14	-0.8660254	-0.1000000	0.52915	0.00000	-2.26779	1.88982
15	-0.7071068	-0.1414214	0.72111	0.43070	-1.60740	1.38675
16	-0.5000000	-0.1732051	0.87178	0.68825	-1.19208	1.14708
17	-0.2588190	-0.1931852	0.96731	0.87720	-0.87720	1.03379
18	0.0000000	-0.2000000	1.00000	1.03923	-0.60000	1.00000
19	0.2588190	-0.1931852	0.96731	1.19828	-0.32108	1.03379
20	0.5000000	-0.1732051	0.87178	1.37649	0.00000	1.14708
21	0.7071068	-0.1414214	0.72111	1.60740	0.43070	1.38675
22	0.8660254	-0.1000000	0.52915	1.96396	1.13389	1.88982
23	0.9659258	-0.0517638	0.32297	2.62729	2.62729	3.09629

TABLE 2. Coordinates and fundamental solutions using procedure A for a 20% thick single ellipse at an angle of attack $\alpha_s = 30°$.

ν	x_ν	y_ν	$\dot{s}_\nu$	$v_\nu^{(1)}$	$v_\nu^{(2)}$	$v_\nu^{(3)}$
0	1.0000000	0.0000000	0.20000	3.00116	5.19816	5.00000
1	0.9659258	0.0517638	0.32297	0.96241	3.59011	3.09629
2	0.8660254	0.1000000	0.52915	0.00046	2.26840	1.88982
3	0.7071068	0.1414214	0.72111	-0.43039	1.60775	1.38675
4	0.5000000	0.1732051	0.87178	-0.68803	1.19226	1.14708
5	0.2588190	0.1931852	0.96731	-0.87706	0.87726	1.03379
6	0.0000000	0.2000000	1.00000	-1.03915	0.59995	1.00000
7	-0.2588190	0.1931852	0.96731	-1.19826	0.32092	1.03379
8	-0.5000000	0.1732051	0.87178	-1.37655	-0.00028	1.14708
9	-0.7071068	0.1414214	0.72111	-1.60755	-0.43114	1.38675
10	-0.8660254	0.1000000	0.52915	-1.96426	-1.13459	1.88982
11	-0.9659258	0.0517638	0.32297	-2.62792	-2.62853	3.09629
12	-1.0000000	0.0000000	0.20000	-3.00116	-5.19816	5.00000
13	-0.9659258	-0.0517638	0.32297	-0.96241	-3.59011	3.09629
14	-0.8660254	-0.1000000	0.52915	-0.00046	-2.26840	1.88982
15	-0.7071068	-0.1414214	0.72111	0.43039	-1.60775	1.38675
16	-0.5000000	-0.1732051	0.87178	0.68803	-1.19226	1.14708
17	-0.2588190	-0.1931852	0.96731	0.87706	-0.87726	1.03379
18	0.0000000	-0.2000000	1.00000	1.03915	-0.59995	1.00000
19	0.2588190	-0.1931852	0.96731	1.19826	-0.32092	1.03379
20	0.5000000	-0.1732051	0.87178	1.37655	0.00028	1.14708
21	0.7071068	-0.1414214	0.72111	1.60755	0.43114	1.38675
22	0.8660254	-0.1000000	0.52915	1.96426	1.13459	1.88982
23	0.9659258	-0.0517638	0.32297	2.62792	2.62853	3.09629

TABLE 3. Coordinates and fundamental solutions using procedure B for a 20% thick single ellipse at an angle of attack $\alpha_s = 30°$.

	x_ν	y_ν	$\dot{s}_\nu$	$v_\nu^{(1)}$	$v_\nu^{(2)}$	$v_\nu^{(3)}$
0	1.0000000	0.0000000	0.20000	3.00009	5.19631	5.00000
1	0.9659258	0.0517638	0.32297	0.96183	3.58896	3.09629
2	0.8660254	0.1000000	0.52915	0.00017	2.26775	1.88982
3	0.7071068	0.1414214	0.72111	-0.43053	1.60734	1.38675
4	0.5000000	0.1732051	0.87178	-0.68808	1.19201	1.14708
5	0.2588190	0.1931852	0.96731	-0.87704	0.87712	1.03379
6	0.0000000	0.2000000	1.00000	-1.03908	0.59991	1.00000
7	-0.2588190	0.1931852	0.96731	-1.19813	0.32098	1.03379
8	-0.5000000	0.1732051	0.87178	-1.37635	-0.00011	1.14708
9	-0.7071068	0.1414214	0.72111	-1.60727	-0.43082	1.38675
10	-0.8660254	0.1000000	0.52915	-1.96384	-1.13403	1.88982
11	-0.9659258	0.0517638	0.32297	-2.62722	-2.62745	3.09629
12	-1.0000000	0.0000000	0.20000	-3.00009	-5.19631	5.00000
13	-0.9659258	-0.0517638	0.32297	-0.96183	-3.58896	3.09629
14	-0.8660254	-0.1000000	0.52915	-0.00017	-2.26775	1.88982
15	-0.7071068	-0.1414214	0.72111	0.43053	-1.60734	1.38675
16	-0.5000000	-0.1732051	0.87178	0.68808	-1.19201	1.14708
17	-0.2588190	-0.1931852	0.96731	0.87704	-0.87712	1.03379
18	0.0000000	-0.2000000	1.00000	1.03908	-0.59991	1.00000
19	0.2588190	-0.1931852	0.96731	1.19813	-0.32098	1.03379
20	0.5000000	-0.1732051	0.87178	1.37635	0.00011	1.14708
21	0.7071068	-0.1414214	0.72111	1.60726	0.43082	1.38675
22	0.8660254	-0.1000000	0.52915	1.96384	1.13403	1.88982
23	0.9659258	-0.0517638	0.32297	2.62722	2.62745	3.09629

TABLE 4. Coordinates and fundamental solutions using procedure A for a cascade of 20% thick elliptical contours with the pitch ratio equal to 1.0, at an angle of attack $\alpha_s = 30°$.

ν	x_ν	y_ν	$\dot{s}_\nu$	$v_\nu^{(1)}$	$v_\nu^{(2)}$	$v_\nu^{(3)}$
0	1.0000000	0.0000000	0.20000	2.65278	4.03213	6.56070
1	0.9659258	0.0517638	0.32297	0.61760	2.76939	4.46483
2	0.8660254	0.1000000	0.52915	-0.28272	1.71578	2.76477
3	0.7071068	0.1414214	0.72111	-0.69331	1.16664	1.89483
4	0.5000000	0.1732051	0.87178	-0.95337	0.80452	1.33927
5	0.2588190	0.1931852	0.96731	-1.15457	0.52683	0.94268
6	0.0000000	0.2000000	1.00000	-1.32438	0.29861	0.67333
7	-0.2588190	0.1931852	0.96731	-1.47200	0.09875	0.54733
8	-0.5000000	0.1732051	0.87178	-1.61238	-0.10933	0.59990
9	-0.7071068	0.1414214	0.72111	-1.78155	-0.39549	0.89822
10	-0.8660254	0.1000000	0.52915	-2.05236	-0.90329	1.62716
11	-0.9659258	0.0517638	0.32297	-2.56998	-2.04295	3.41399
12	-1.0000000	0.0000000	0.20000	-2.65278	-4.03213	6.56070
13	-0.9659258	-0.0517638	0.32297	-0.61760	-2.76939	4.46483
14	-0.8660254	-0.1000000	0.52915	0.28272	-1.71578	2.76477
15	-0.7071068	-0.1414214	0.72111	0.69331	-1.16664	1.89483
16	-0.5000000	-0.1732051	0.87178	0.95337	-0.80452	1.33927
17	-0.2588190	-0.1931852	0.96731	1.15457	-0.52683	0.94268
18	0.0000000	-0.2000000	1.00000	1.32438	-0.29861	0.67333
19	0.2588190	-0.1931852	0.96731	1.47200	-0.09875	0.54733
20	0.5000000	-0.1732051	0.87178	1.61238	0.10933	0.59990
21	0.7071068	-0.1414214	0.72111	1.78155	0.39549	0.89822
22	0.8660254	-0.1000000	0.52915	2.05236	0.90329	1.62716
23	0.9659258	-0.0517638	0.32297	2.56998	2.04295	3.41399

TABLE 5. Coordinates and fundamental solutions using procedure B for a cascade of 20% thick elliptical contours with the pitch ratio equal to 1.0, at an angle of attack $\alpha_s = 30°$.

ν	x_ν	y_ν	$\dot{s}_\nu$	$v_\nu^{(1)}$	$v_\nu^{(2)}$	$v_\nu^{(3)}$
0	1.0000000	0.0000000	0.20000	2.65199	4.03099	6.56037
1	0.9659258	0.0517638	0.32297	0.61723	2.76872	4.46461
2	0.8660254	0.1000000	0.52915	-0.28286	1.71543	2.76466
3	0.7071068	0.1414214	0.72111	-0.69333	1.16646	1.89479
4	0.5000000	0.1732051	0.87178	-0.95331	0.80444	1.33928
5	0.2588190	0.1931852	0.96731	-1.15445	0.52684	0.94273
6	0.0000000	0.2000000	1.00000	-1.32421	0.29869	0.67341
7	-0.2588190	0.1931852	0.96731	-1.47179	0.09888	0.54741
8	-0.5000000	0.1732051	0.87178	-1.61213	-0.10914	0.59997
9	-0.7071068	0.1414214	0.72111	-1.78125	-0.39523	0.89825
10	-0.8660254	0.1000000	0.52915	-2.05197	-0.90289	1.62714
11	-0.9659258	0.0517638	0.32297	-2.56941	-2.04226	3.41384
12	-1.0000000	0.0000000	0.20000	-2.65199	-4.03099	6.56037
13	-0.9659258	-0.0517638	0.32297	-0.61723	-2.76872	4.46461
14	-0.8660254	-0.1000000	0.52915	0.28286	-1.71543	2.76466
15	-0.7071068	-0.1414214	0.72111	0.69333	-1.16646	1.89479
16	-0.5000000	-0.1732051	0.87178	0.95331	-0.80444	1.33928
17	-0.2588190	-0.1931852	0.96731	1.15445	-0.52684	0.94273
18	0.0000000	-0.2000000	1.00000	1.32421	-0.29869	0.67341
19	0.2588190	-0.1931852	0.96731	1.47179	-0.09688	0.54741
20	0.5000000	-0.1732051	0.87178	1.61213	0.10914	0.59997
21	0.7071068	-0.1414214	0.72111	1.78125	0.39523	0.89825
22	0.8660254	-0.1000000	0.52915	2.05197	0.90289	1.62714
23	0.9659258	-0.0517638	0.32297	2.56941	2.04226	3.41384

TABLE 6. Coordinates and fundamental solutions using procedure A for a cascade using contour No. 9 with pitch ratio 1.0, at an angle of attack $\alpha_s = 40°$.

ν	x_ν	y_ν	$\dot{s}_\nu$	$v_\nu^{(1)}$	$v_\nu^{(2)}$	$v_\nu^{(3)}$
0	0.9992000	0.0011000	0.01772	13.12884	6.35601	21.44227
1	0.9877000	0.0168000	0.14368	-9.19287	-2.68695	-9.07411
2	0.9480000	0.0540000	0.27122	2.91501	2.05747	6.68050
3	0.8806000	0.1090000	0.38955	3.41342	1.58176	5.07616
4	0.7889000	0.1769000	0.47799	0.59877	1.31449	4.22795
5	0.6780000	0.2529000	0.54412	0.01610	1.17992	3.73079
6	0.5524000	0.3289000	0.57134	-0.48377	1.04014	3.30015
7	0.4193000	0.3960000	0.55883	-1.15351	0.89762	2.91561
8	0.2850000	0.4279000	0.50321	-2.21244	0.54864	2.15021
9	0.1625000	0.3976000	0.46855	-2.58026	0.00501	1.49058
10	0.0710000	0.3273000	0.42169	-2.38235	-0.48263	2.12001
11	0.0170000	0.2368000	0.37966	-1.87626	-1.01275	3.48586
12	0.0000000	0.1510000	0.29398	-1.31187	-1.60843	5.29746
13	0.0155000	0.0821000	0.25801	-0.50998	-2.00905	6.54315
14	0.0575000	0.0310000	0.25956	0.40968	-2.01880	6.56958
15	0.1231000	0.0024000	0.29878	1.26563	-1.70812	5.61329
16	0.2145000	0.0170000	0.43682	1.44211	-0.86805	2.97636
17	0.3347000	0.0682000	0.53395	1.20191	-0.36562	1.38960
18	0.4713000	0.1009000	0.54022	1.27164	-0.20600	0.93765
19	0.6119000	0.1087000	0.52872	1.48617	-0.08848	0.77702
20	0.7424000	0.0945000	0.47033	1.81352	0.03095	0.81334
21	0.8510000	0.0641000	0.38726	2.57623	0.28866	1.45509
22	0.9323000	0.0330000	0.27299	3.91447	0.83235	3.10944
23	0.9812000	0.0089000	0.14284	-8.53086	-3.87085	-12.60546

TABLE 7. Coordinates and fundamental solutions using procedure B for a cascade using contour No. 9 with pitch ratio 1.0, at an angle of attack $\alpha_s = 40°$.

ν	x_ν	y_ν	$\dot{s}_\nu$	$v_\nu^{(1)}$	$v_\nu^{(2)}$	$v_\nu^{(3)}$
0	0.9992000	0.0011000	0.01772	37.69728	11.64376	38.13269
1	0.9877000	0.0168000	0.14368	3.56773	1.84881	5.92096
2	0.9480000	0.0540000	0.27122	1.26393	1.28465	4.08919
3	0.8806000	0.1090000	0.38955	0.33291	1.10863	3.50984
4	0.7889000	0.1769000	0.47799	-0.16430	1.03142	3.25466
5	0.6780000	0.2529000	0.54412	-0.62147	0.94657	2.98701
6	0.5524000	0.3289000	0.57134	-1.15035	0.81358	2.58061
7	0.4193000	0.3960000	0.55883	-2.08929	0.58726	1.93000
8	0.2850000	0.4279000	0.50321	-3.23053	0.21872	1.10587
9	0.1625000	0.3976000	0.46855	-3.14004	-0.18241	0.90001
10	0.0710000	0.3273000	0.42169	-2.63424	-0.56694	1.86857
11	0.0170000	0.2368000	0.37966	-2.02799	-1.06606	3.31108
12	0.0000000	0.1510000	0.29398	-1.43435	-1.65006	5.19100
13	0.0155000	0.0821000	0.25801	-0.63046	-2.04477	6.41553
14	0.0575000	0.0310000	0.25956	0.29985	-2.05118	6.50051
15	0.1231000	0.0024000	0.29878	1.15424	-1.73264	5.51976
16	0.2145000	0.0170000	0.43682	1.33547	-0.89292	2.12402
17	0.3347000	0.0682000	0.53395	1.11637	-0.37605	1.34830
18	0.4713000	0.1009000	0.54022	1.18476	-0.21340	0.92670
19	0.6119000	0.1087000	0.52872	1.37230	-0.08893	0.74217
20	0.7424000	0.0945000	0.47033	1.64536	0.02994	0.77741
21	0.8510000	0.0641000	0.38726	2.20081	0.20389	1.09959
22	0.9323000	0.0330000	0.27299	2.96024	0.45854	1.77294
23	0.9812000	0.0089000	0.14284	5.24010	1.14526	3.89806

TABLE 8. Coordinates and fundamental solutions using procedure B for a cascade using contour No. 10 with pitch ratio 1.0, at an angle of attack $\alpha_s = 40°$.

ν	x_ν	y_ν	$\dot{s}_\nu$	$v_\nu^{(1)}$	$v_\nu^{(2)}$	$v_\nu^{(3)}$
0	0.9993000	0.0013000	0.01632	38.75262	13.09774	42.98791
1	0.9870000	0.0161000	0.14283	3.24950	1.79803	5.78114
2	0.9462000	0.0520000	0.27065	1.14987	1.23524	3.94024
3	0.8797000	0.1070000	0.38547	0.34619	1.13135	3.59244
4	0.7878000	0.1738000	0.47886	-0.17430	1.03952	3.28696
5	0.6762000	0.2487000	0.54096	-0.63922	0.95147	3.01047
6	0.5509000	0.3220000	0.56321	-1.23809	0.82549	2.63015
7	0.4155000	0.3780000	0.54935	-2.08386	0.54699	1.84001
8	0.2808000	0.3994000	0.49560	-2.96166	0.18119	1.05685
9	0.1607000	0.3699000	0.45859	-2.97790	-0.19227	1.00905
10	0.0701000	0.3030000	0.40250	-2.57497	-0.59296	1.95930
11	0.0172000	0.2209000	0.34995	-2.07299	-1.11039	3.48879
12	0.0000000	0.1390000	0.29170	-1.46601	-1.70277	5.35685
13	0.0159000	0.0713000	0.25097	-0.61364	-2.12962	6.70415
14	0.0587000	0.0235000	0.25284	0.34280	-2.05679	6.64272
15	0.1259000	0.0004000	0.30446	1.12108	-1.64222	5.24750
16	0.2185000	0.0165000	0.43150	1.26588	-0.85776	2.81777
17	0.3380000	0.0629000	0.52802	1.10984	-0.39104	1.39926
18	0.4745000	0.0950000	0.53918	1.15905	-0.21596	0.94097
19	0.6140000	0.1033000	0.52388	1.32910	-0.09451	0.75926
20	0.7440000	0.0907000	0.46843	1.56536	0.02991	0.78995
21	0.8519000	0.0620000	0.38121	2.06146	0.20363	1.12590
22	0.9321000	0.0314000	0.27075	2.87368	0.50706	1.95443
23	0.9814000	0.0087000	0.14216	5.12538	1.27646	4.36522

TABLE 9. Coordinates and fundamental solutions using procedure B for a cascade using contour No. 12 with pitch ratio 1.0, at an angle of attack $\alpha_s = 40°$.

ν	x_ν	y_ν	$\dot{s}_\nu$	$v_\nu^{(1)}$	$v_\nu^{(2)}$	$v_\nu^{(3)}$
0	0.9993000	0.0011000	0.01879	31.11854	10.23128	34.08404
1	0.9886000	0.0175000	0.14406	3.12023	1.72565	5.58351
2	0.9507000	0.0570000	0.27376	1.30847	1.33220	4.24986
3	0.8879000	0.1189000	0.39616	0.45421	1.20684	3.83439
4	0.8000000	0.1953000	0.48934	-0.10702	1.16994	3.70265
5	0.6885000	0.2750000	0.55118	-0.71061	1.05164	3.34226
6	0.5573000	0.3415000	0.56737	-1.43778	0.85039	2.73334
7	0.4153000	0.3775000	0.54992	-2.24461	0.46136	1.66382
8	0.2767000	0.3723000	0.51347	-2.71015	0.07539	0.96885
9	0.1569000	0.3259000	0.46682	-2.53411	-0.26705	1.16685
10	0.0688000	0.2580000	0.38448	-2.29713	-0.67450	2.24471
11	0.0170000	0.1812000	0.33077	-1.92031	-1.23455	3.91729
12	0.0000000	0.1060000	0.26044	-1.36916	-1.91326	6.04813
13	0.0157000	0.0456000	0.22977	-0.44097	-2.39772	7.57305
14	0.0581000	0.0060000	0.23029	0.69703	-2.45255	7.76483
15	0.1275000	0.0083000	0.34313	1.30706	-1.43418	4.59496
16	0.2293000	0.0747000	0.57771	0.91568	-0.50313	1.66119
17	0.3612000	0.1502000	0.54427	0.64737	-0.20736	0.77785
18	0.4956000	0.1526000	0.51243	0.86079	-0.19748	0.77831
19	0.6269000	0.1287000	0.50085	1.16605	-0.14432	0.75168
20	0.7479000	0.0946000	0.45558	1.49237	-0.06510	0.71421
21	0.8514000	0.0584000	0.37668	2.04776	0.08416	0.94807
22	0.9310000	0.0278000	0.27057	2.75786	0.34500	1.57397
23	0.9810000	0.0070000	0.14064	5.33618	1.20478	4.30404

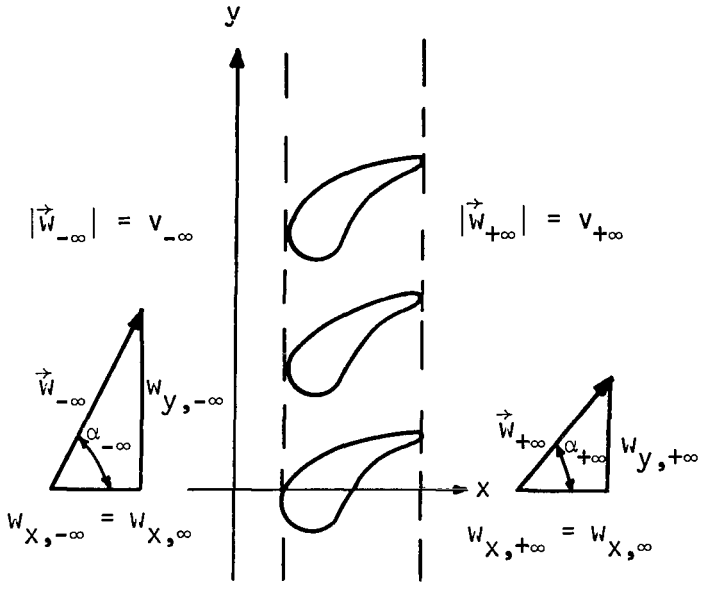

FIGURE 5. Labeling of the pertinent quantities far upstream and downstream.

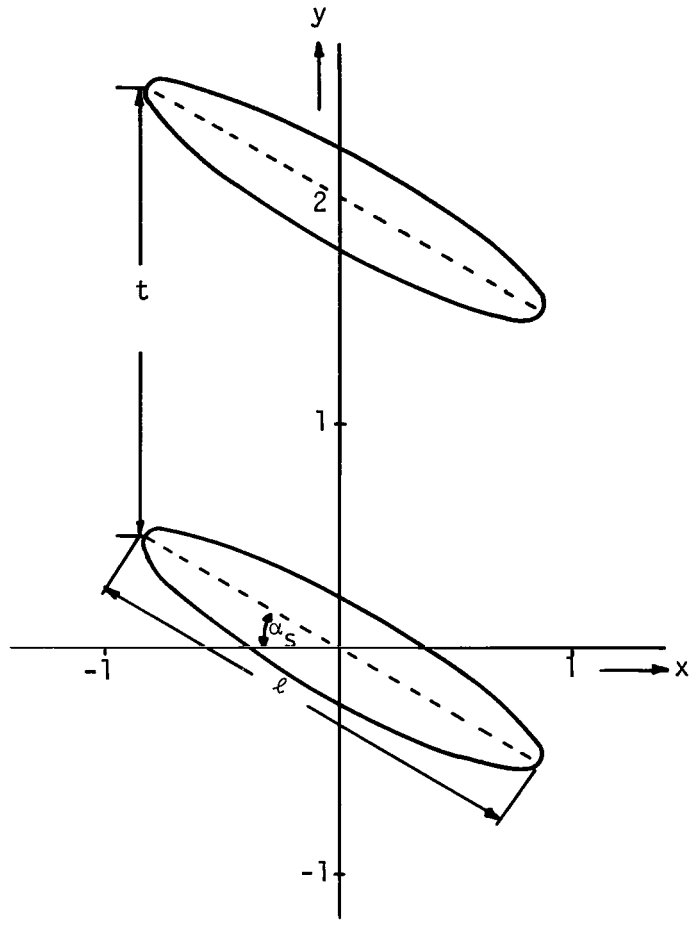

FIGURE 6. Cascade of 20% thick ellipses at pitch ratio, $t/\ell = 1$, and at an angle of attack, $\alpha_s = 30°$.

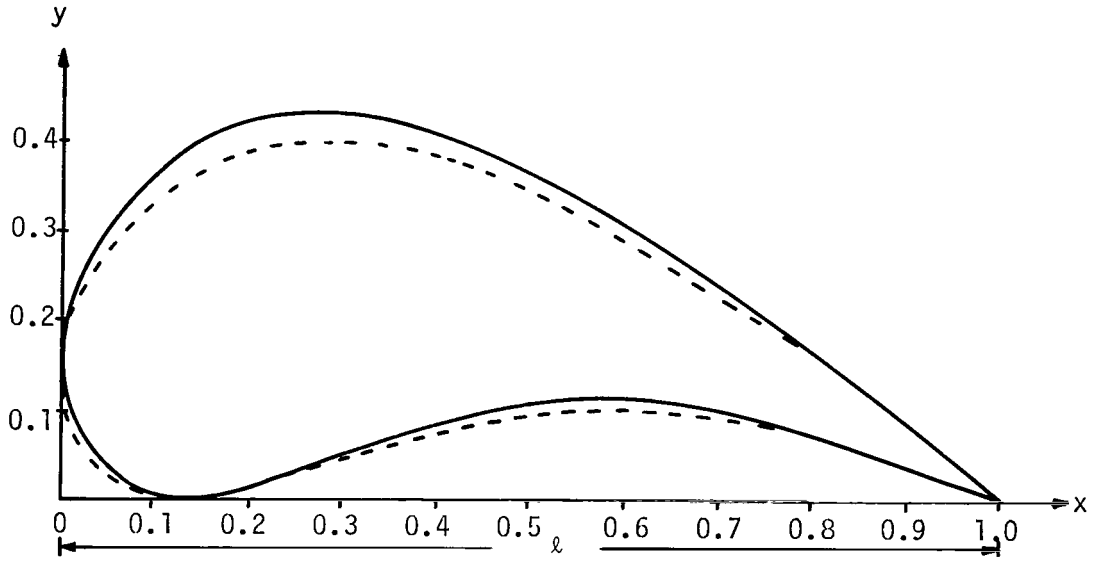

FIGURE 7. Contour No. 9 (————) and 10 (-------).

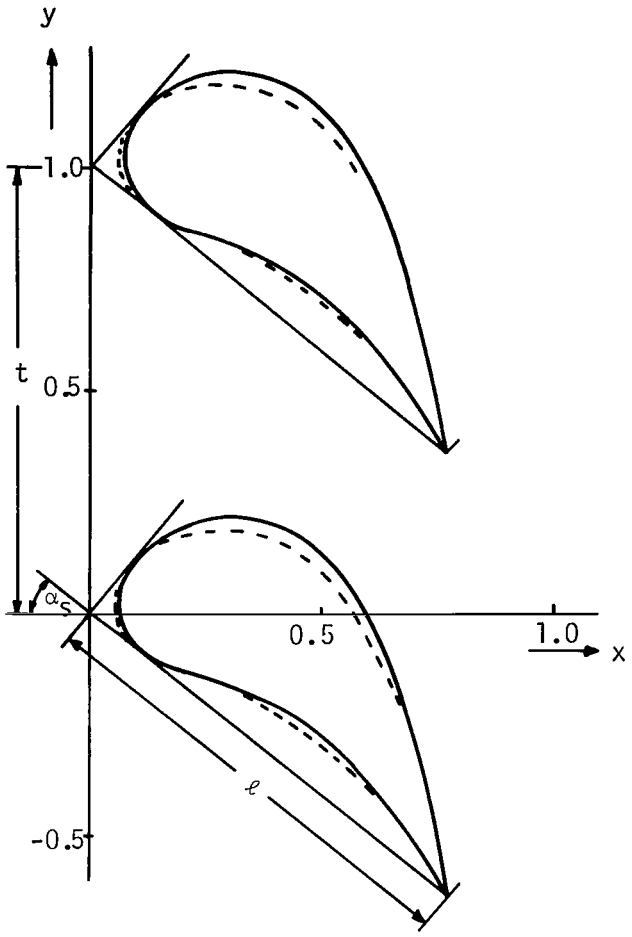

FIGURE 8. Contour Nos. 9 (————) and 10 (--------) with pitch ratio $t/\ell = 1$ and $\alpha_s = 40°$.

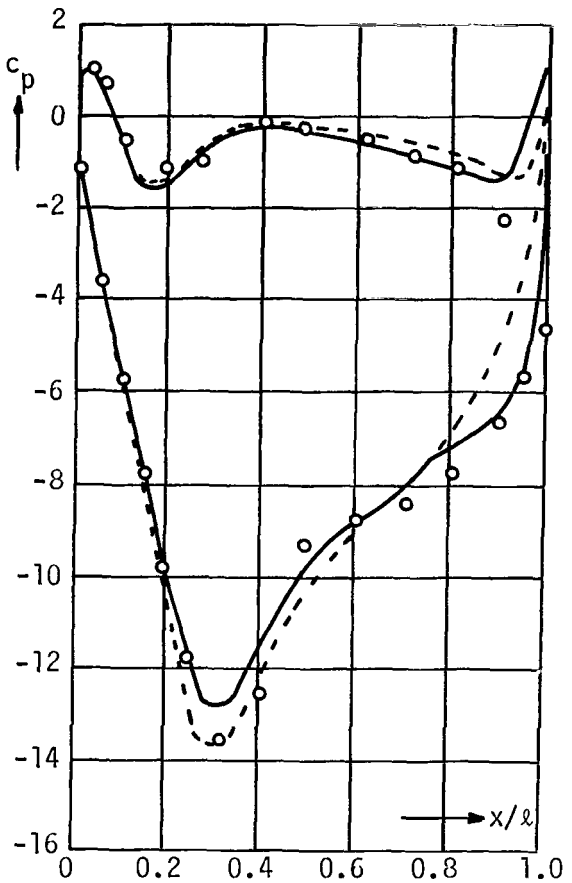

FIGURE 9. Comparison between the theoretical and measured pressure distribution for contour No. 9 with $t/\ell = 1$, $\alpha_s = 40°$, $\alpha_{-\infty} = -15°$, $\alpha_{+\infty} = -69.6°$. Solid line, method A; dashed line, method B; circles, measured values according to [13].

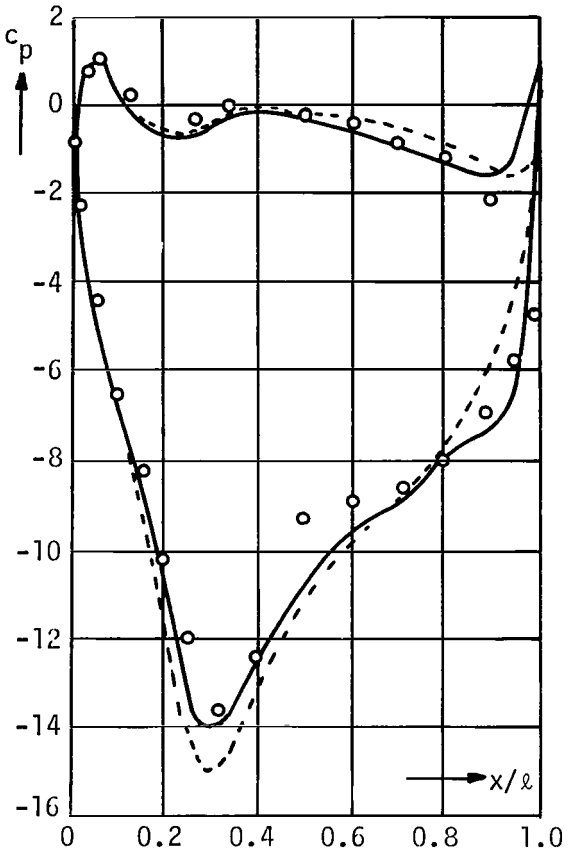

FIGURE 10. Comparison between the theoretical and measured pressure distribution for contour No. 9 with $t/\ell = 1$, $\alpha_s = 40°$, $\alpha_{-\infty} = 0°$, $\alpha_{+\infty} = -69.6°$. Solid line, method A; dashed line, method B; circles, measured values according to [13].

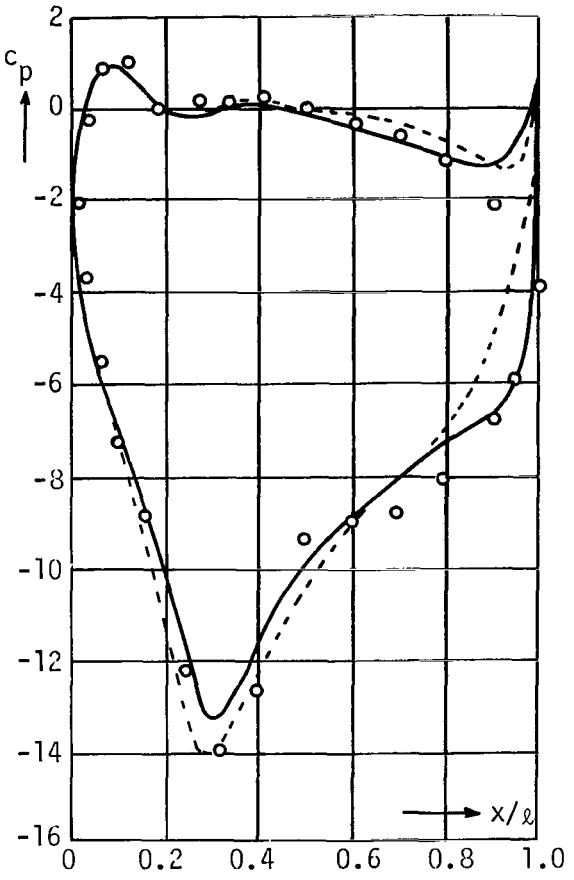

FIGURE 11. Comparison between the theoretical and measured pressure distribution for contour No. 9 with $t/\ell = 1$, $\alpha_s = 40°$, $\alpha_{-\infty} = 15°$, $\alpha_{+\infty} = -69.6°$. Solid line, method A; dashed line, method B; circles, measured values according to [13].

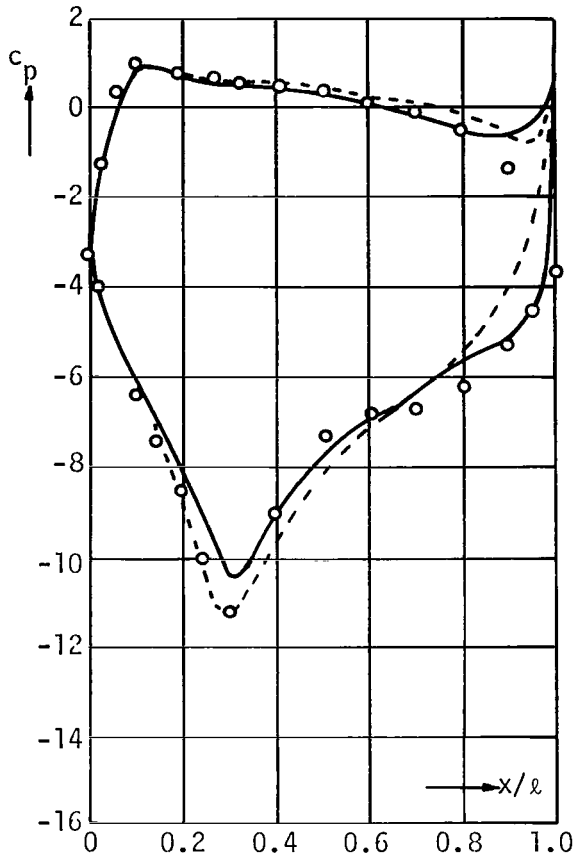

FIGURE 12. Comparison between the theoretical and measured pressure distribution for contour No. 9 with $t/\ell = 1$, $\alpha_s = 40°$, $\alpha_{-\infty} = 30°$, $\alpha_{+\infty} = -69.6°$. Solid line, method A; dashed line, method B; circles, measured values according to [13].

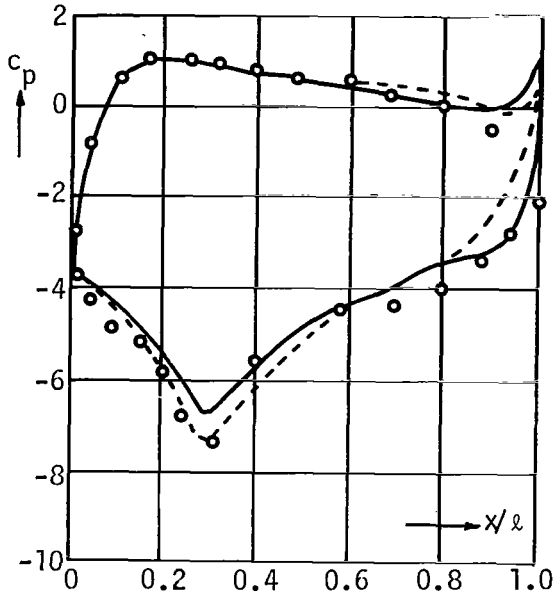

FIGURE 13. Comparison between the theoretical and measured pressure distribution for contour No. 9 with $t/\ell = 1$, $\alpha_s = 40°$, $\alpha_{-\infty} = 45°$, $\alpha_{+\infty} = -69.6°$. Solid line, method A; dashed line, method B; circles, measured values according to [13].

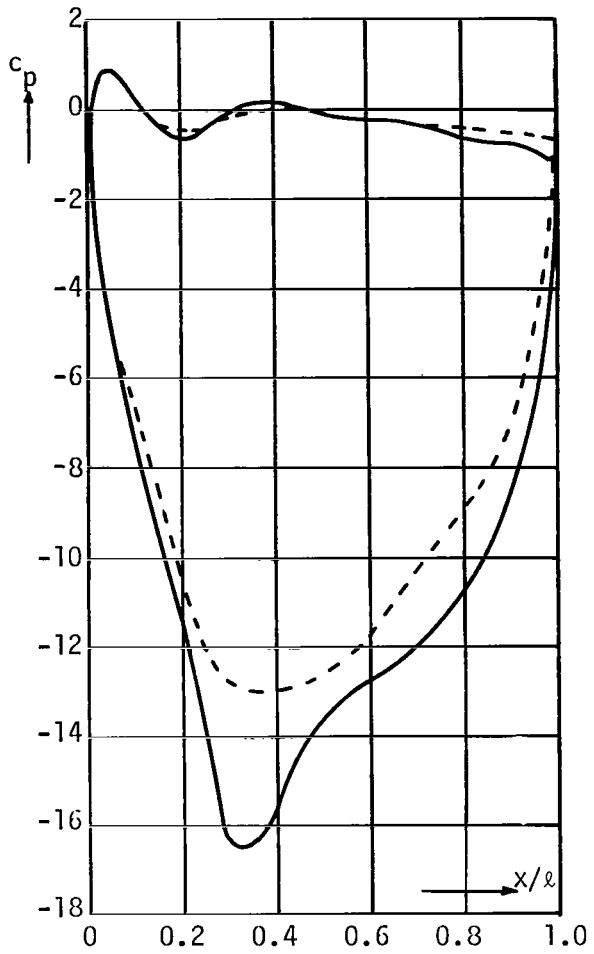

FIGURE 14. Theoretical pressure distribution using procedure B for the contour Nos. 9 (————) and 10 (-------), $t/\ell = 1$, $\alpha_s = 40°$, $\alpha_{-\infty} = 0°$, and $\alpha_{+\infty} = -72.5°$ for contour 9 and -70.9° for contour 10 (stagnation point at trailing edge).

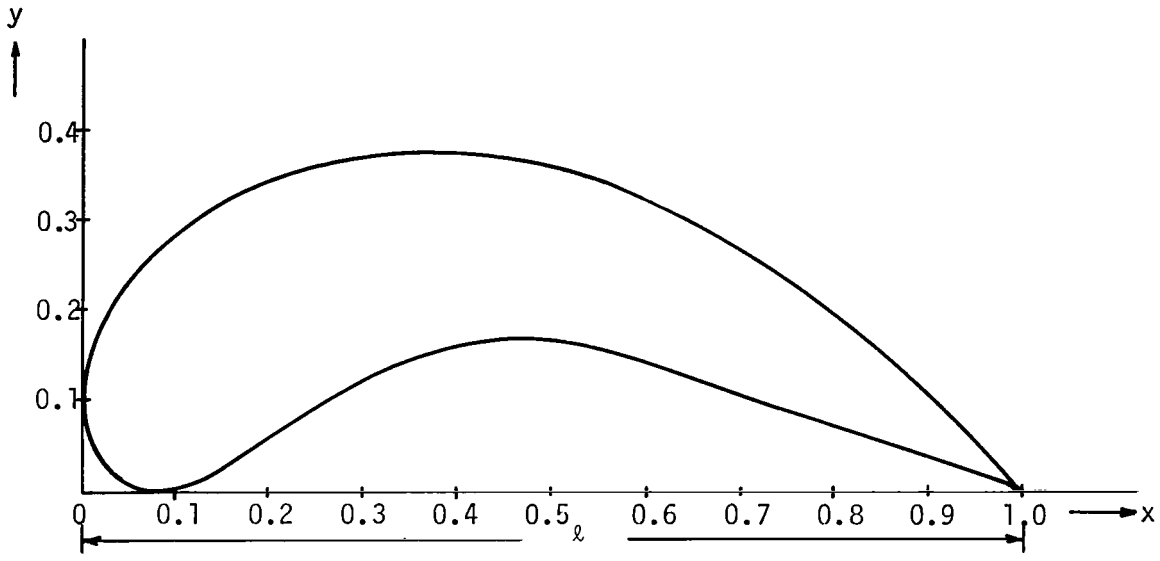

FIGURE 15. Contour No. 12.

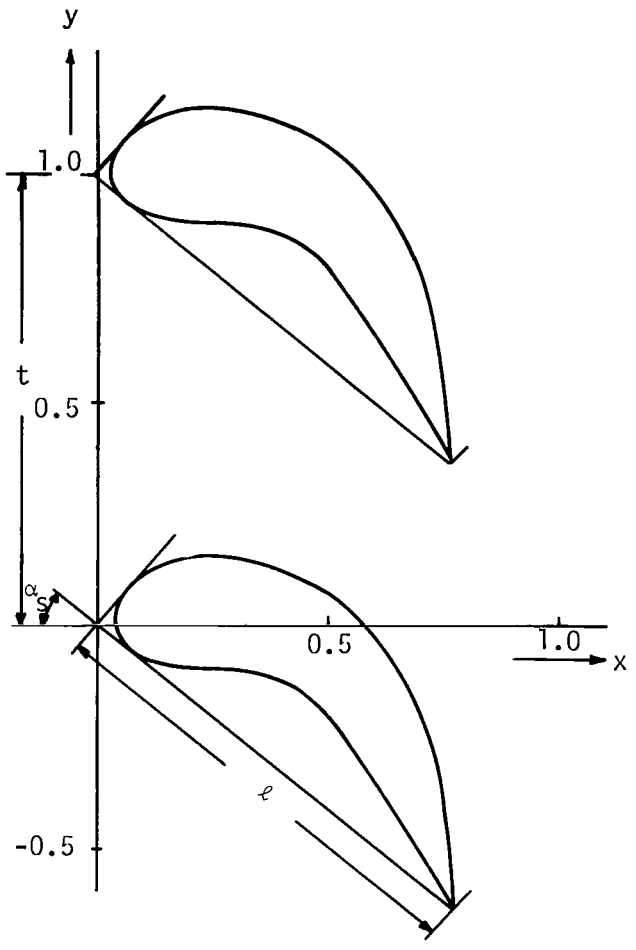

FIGURE 16. Contour No. 12, with the pitch ratio $t/\ell = 1.0$, and $\alpha_s = 40°$.

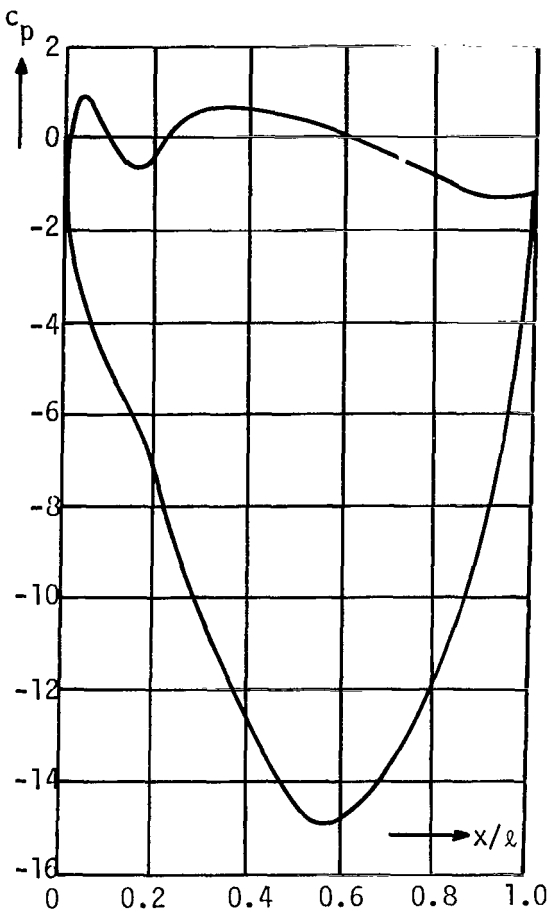

FIGURE 17. Theoretical pressure distribution using procedure B for contour No. 12 with $t/\ell = 1$, $\alpha_s = 40°$, $\alpha_{-\infty} = 0°$, $\alpha_{+\infty} = -71.3°$ (stagnation point at trailing edge).

NASA-Langley, 1971 —— 1 F-702